


## RESEARCH ARTICLE

# IGF-1 regulates astrocytic phagocytosis and inflammation through the p110 $\alpha$ isoform of PI3K in a sex-specific manner

Daniel Pinto-Benito<sup>1,2</sup>  | Carmen Paradela-Leal<sup>1</sup> | Danny Ganchala<sup>1</sup> |  
Paula de Castro-Molina<sup>1</sup> | Maria-Angeles Arevalo<sup>1,2</sup> 

<sup>1</sup>Consejo Superior de Investigaciones Científicas (CSIC), Instituto Cajal, Madrid, Spain

<sup>2</sup>Centro de Investigación Biomédica en Red de Fragilidad y Envejecimiento Saludable (CIBERFES), Instituto de Salud Carlos III, Madrid, Spain

**Correspondence**

Maria-Angeles Arevalo, Consejo Superior de Investigaciones Científicas (CSIC), Instituto Cajal, Madrid, Spain.  
Email: arevalo@cajal.csic.es

**Funding information**

Centro de Investigación Biomédica en Red Fragilidad y Envejecimiento Saludable; Ministerio de Ciencia e Innovación, Grant/Award Numbers: BFU2017-82754-R, PID2020-115019RB-I00; Fondo Europeo de Desarrollo Regional (FEDER); Agencia Estatal de Investigación (AEI)

**Abstract**

Insulin-like growth factor-I (IGF-I) signaling plays a key role in neuroinflammation. Here we show that IGF-1 also regulates phagocytosis of reactive astrocytes through p110 $\alpha$  isoform of phosphatidylinositol 3-kinase (PI3K), differentially in both sexes. Systemic bacterial lipopolysaccharide (LPS)-treatment increased the expression of GFAP, a reactive astrocyte marker, in the cortex of mice in both sexes and was blocked by IGF-1 only in males. In primary astrocytes, LPS enhanced the mRNA expression of Toll-like receptors (TLR2,4) and proinflammatory factors: inducible nitric oxide synthase (iNOS), chemokine interferon- $\gamma$ -inducible protein-10 (IP-10) and cytokines (IL-1 $\beta$ , IL-6, and IL-10) in male and female. Treatment with IGF-1 counteracted TLR4 but not TLR2, iNOS, and IP10 expression in both sexes and cytokines expression in males. Furthermore, reactive astrocyte phagocytosis was modulated by IGF-1 only in male astrocytes. IGF-1 was also able to increase AKT-phosphorylation only in male astrocytes. PI3K inhibitors, AG66, TGX-221, and CAL-101, with selectivity toward catalytic p110 $\alpha$ , p110 $\beta$ , and p110 $\delta$  isoforms respectively, reduced AKT-phosphorylation in males. All isoforms interact physically with IGF-1-receptor in both sexes. However, the expression of p110 $\alpha$  is higher in males while the expression of IGF-1-receptor is similar in male and female. AG66 suppressed the IGF-1 effect on cytokine expression and counteracted the IGF-1-produced phagocytosis decrease in male reactive astrocytes. Results suggest that sex-differences in the effect of IGF-1 on the AKT-phosphorylation could be due to a lower expression of the p110 $\alpha$  in female and that IGF-1-effects on the inflammatory response and phagocytosis of male reactive astrocytes are mediated by p110 $\alpha$ /PI3K subunit.

**KEYWORDS**

IGF-1, neuroinflammation, phagocytosis, PI3K-isoforms, sex differences

This is an open access article under the terms of the Creative Commons Attribution-NonCommercial-NoDerivs License, which permits use and distribution in any medium, provided the original work is properly cited, the use is non-commercial and no modifications or adaptations are made.

© 2022 The Authors. GLIA published by Wiley Periodicals LLC.



## 1 | INTRODUCTION

Sexual dimorphism in response to bacterial infections has been extensively described in hospital environments, where it has been observed that men were more susceptible to bacteremia than women (Bösch et al., 2018; McGowan Jr. et al., 1975) and mortality was less common in women after a septic infection than men (Kondo et al., 2021). In the context of central nervous system (CNS), numerous neurological and psychiatric disorders show sex differences in incidence, age of onset, symptomatology or outcome and most of these disorders course with neuroinflammation (Giatti et al., 2020). Even in physiological aging, neuroinflammation contributes to age-related cognitive decline in a sex-dependent manner (Porcher et al., 2021). These findings suggest sex differences in the response of glial cells to inflammatory and neurodegenerative conditions. Astrocytes play key roles in the response of the nerve tissue to damage (Liddelow et al., 2017). When the brain is infected or injured, astrocytes undergo a transformation called “reactive astrogliosis”. Reactive astrocytes show many up-regulated genes and form a glial scar after acute CNS trauma (Anderson et al., 2014; Sofroniew & Vinters, 2010). Functions of reactive astrocytes have been a subject of some debate; it has not been clarified under what contexts they may be beneficial or detrimental, and many questions remain unsolved about their actions.

In addition, astrocytes become active participants in the propagation and regulation of neuroinflammation. They act by removing cell debris and denatured proteins to facilitate tissue repair. This process is named “phagocytosis”. Astrocytic phagocytosis achieves physiological neuronal synaptic pruning during development and adulthood (Bellesi et al., 2017; Chung et al., 2013; Chung et al., 2016; Jung & Chung, 2018) and contributes to the remodeling of myelin and the clearance of cellular debris under pathological conditions (Jung & Chung, 2018; Morizawa et al., 2017; Nguyen et al., 2011; Ponath et al., 2017). Therefore, phagocytosis is essential for the homeostatic function of astrocytes and a reduced phagocytic activity has been identified as an indicator of reactive astrocytes that have lost their neuroprotective function (Liddelow et al., 2017). However, excessive phagocytosis contributes to synaptic loss in some pathologies and could result in secondary neuronal death (Vilalta & Brown, 2018). Therefore, modulation of this process may serve as a promising therapy for some brain disorders.

Systemic bacterial lipopolysaccharide (LPS) administration induces expression of pro-inflammatory genes that have been shown to be detrimental for neuronal survival by activation of NF- $\kappa$ B (Villarreal et al., 2021). In contrast, astrocytes can exert neuroprotective functions by releasing a variety of trophic factors that promote CNS recovery and repair such as insulin like growth factor (IGF)-1 (Chisholm & Sohrabji, 2016). Intraperitoneal LPS injection increases IGF-1 and IGF-1R levels in the mouse brain (Park et al., 2011). IGF-I, a neurotrophic hormone, carries out a broad spectrum of biological activities, including the regulation of immune events. Interactions between IGF-I and the immune system are complex, bidirectional, and have not been fully explained. Evidence suggests that IGF-I could modulate the inflammatory response and the activity of systemic inflammation in males (O'Connor et al., 2008; Witkowska-Sędek & Pyrżak, 2020) and a

cooperation between peripheral and central IGF-1 has been described in a male mouse traumatic brain injury model. Nonetheless, only when additional exogenous administration of IGF-1 was provided, the sensorimotor function was fully restored (Santi et al., 2018). However, it is unknown if astrocyte phagocytosis is also regulated by IGF-1. Thus, in the present study, using primary mouse astrocyte cultures from male and female animals, we have assessed whether IGF-1 regulates astrocytic phagocytosis of neural debris.

The influence of sex on the functions of reactive astrocytes has been little explored. Reactive astrocytes show molecular and morphological sex differences (Acáz-Fonseca et al., 2015; Chisholm & Sohrabji, 2016; Chistyakov et al., 2018; Jaber et al., 2018; Morrison & Filosa, 2016). In addition, previous work from our laboratory showed that the phagocytosis of brain-derived cellular debris was stimulated in male astrocytes but inhibited in females under an inflammatory challenge (Crespo-Castrillo et al., 2020). Here our objective was to evaluate the effect of IGF-1 on neuroinflammation and phagocytosis of male and female astrocytes stimulated with LPS as well as to elucidate the signaling pathways that underlie these processes.

Toll-like receptors (TLRs) are a family of transmembrane proteins of mammalian cells. They are widely expressed in CNS and play key roles in the response of innate immunity cells to pathological stimuli (Brown et al., 2011; Bsibsi et al., 2002). TLR4 activation results in the induction of transcriptional factors such as nuclear factor- $\kappa$ B (NF- $\kappa$ B), which triggers various pro-inflammatory genes for instance those encoding cytokines, chemokines, proteins of the complement system, cyclooxygenase-2, and inducible nitric oxide synthase (iNOS). We and others have previously described that LPS induces the expression of proinflammatory factors by activation of TLR4/NF- $\kappa$ B signaling pathway in astrocytes (Cerciat et al., 2010; Tang et al., 2021) and IGF-I is able to counteract the effect of LPS on cytokine release and on astrocyte morphology by blocking NF- $\kappa$ B signaling (Acáz-Fonseca et al., 2019; Pons & Torres-Aleman, 2000). The main signaling pathways activated by the IGF-1R are Mitogen-activated protein kinase (MAPK) specifically, ERK-1/2 and phosphatidylinositol 3-kinase (PI3-K) pathways and has been described that PI3K activation blocks NF- $\kappa$ B (Khasnavis et al., 2012). In vivo study revealed that IGF-1 improved cognitive function and anxiety behavior in male rats with high-fat diet consumption and inhibited the inflammation and oxidative stress in the hippocampus through the activation of the PI3K/Akt/CREB signaling pathway (Wang et al., 2020).

Mammals express four class I PI3K catalytic isoforms (p110 $\alpha$ ,  $\beta$ ,  $\gamma$ , and  $\delta$ ) that catalyze the phosphorylation of Phosphatidylinositol (4,5)-bisphosphate to generate Phosphatidylinositol (3,4,5)-trisphosphate. The p110 $\alpha$ , p110 $\beta$ , and p110 $\delta$  proteins are expressed ubiquitously, whereas expression of p110 $\gamma$  is restricted to immune cells (Pridham et al., 2018). Despite their high homologies, p110 isoforms regulate distinct physiological and pathological functions (Fruman et al., 2017) but the roles of PI3K isoforms in neuroinflammation remain to be elucidated. Therefore, to investigate the mechanism underlying the actions of IGF-1 on reactive astrocytes, we decided to explore which p110 isoform is involved in the expression of inflammation-related genes and phagocytosis.

## 2 | METHODS

### 2.1 | Animals

CD1 mice raised in our in-house colony at the Cajal Institute were used for this study. Animals were housed under controlled

temperature ( $22 \pm 2^\circ\text{C}$ ) and light (12-h light/dark cycle) conditions and with food and water available ad libitum. All the procedures applied to the animals used in this study followed the European Parliament and Council Directive (2010/63/EU) and the Spanish regulation (R.D. 53/2013 and Ley 6/2013, 11th June) on the protection of animals for experimental use and were approved by our institutional

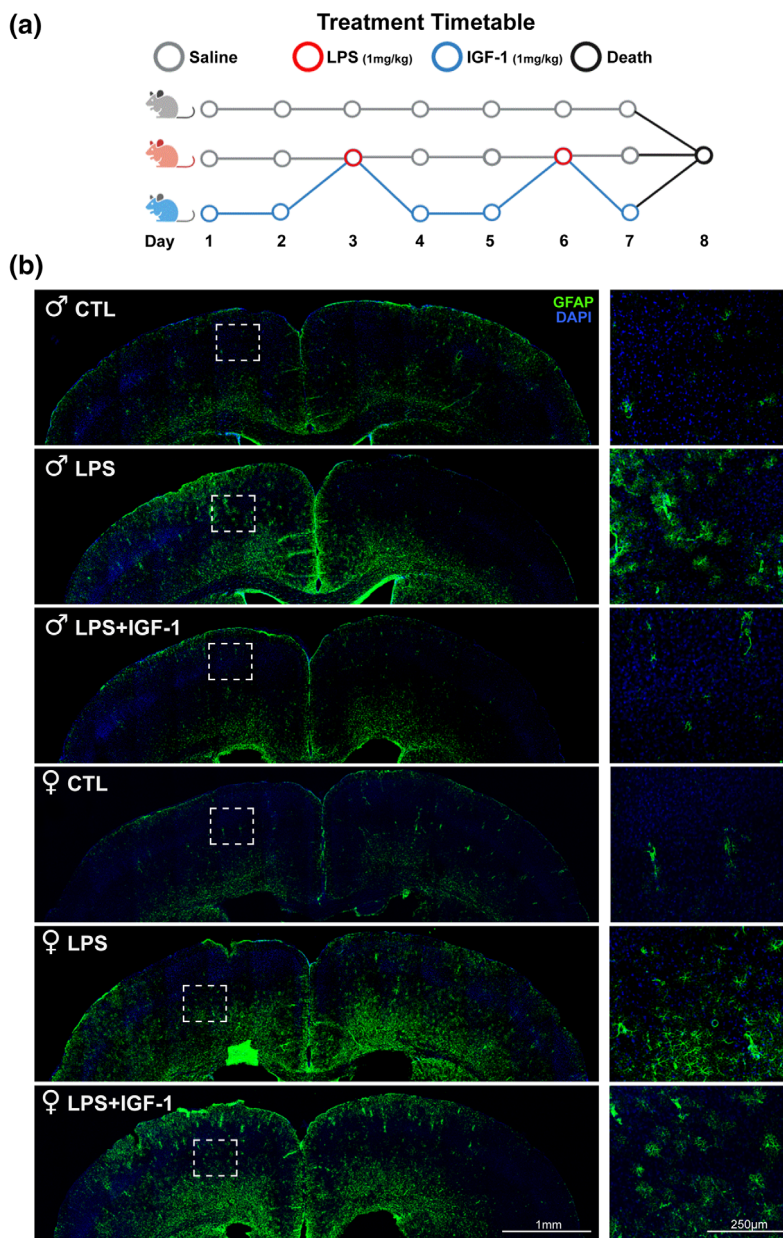
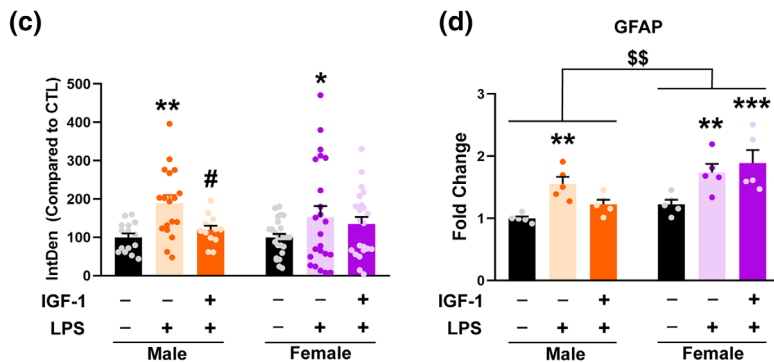


**FIGURE 1** IGF-1 counteracts LPS induced astrogliosis in males. (a) Treatments timetable. Control group received vehicle injections during 7 days. LPS group received vehicle except days 3 and 6 that received LPS. LPS + IGF-1 group were injected with IGF-1 the days that did not receive LPS treatment. (b) Immunofluorescent staining with GFAP (a reactive astrocyte marker) of the of male and female mouse cortex. Representative figures were randomly captured from  $N = 5$  mice/group. (c) Integrated density quantification reveals that astrogliosis induced by LPS treatment is counteracted by IGF-1 treatment only in males. (d) GFAP mRNA expression in the cortex of mice receiving vehicle, LPS or LPS + IGF-1. Data are mean  $\pm$  SEM; two-way ANOVA with Fisher's LSD (c) or Tukey's multiple comparisons (d) test post hoc tests; \* $p < .05$ ; \*\* $p < .01$  versus control groups and # $p < .05$  versus LPS treated groups



animal use and care committee (Comité de Ética de Experimentación Animal del Instituto Cajal) and by the Consejería del Medio Ambiente y Territorio (Comunidad de Madrid, PROEX 134/17). For in vivo experiments, 90 days old male and female mice were injected intraperitoneally (i.p.) with two doses of LPS (1 mg/kg; isotype O55-B5, L2880, Sigma-Aldrich, Tres Cantos, Madrid) as shown previously inducing neuroinflammation (Hasel et al., 2021; Leite et al., 2020; Tapia-Gonzalez et al., 2008) and five doses of IGF-1 (1 mg/kg/day; #100-11, PeproTech, USA) dissolved in 0.9% saline, following the protocol described in Figure 1a, which has been shown to cross the blood-brain barrier and perform actions on the brain (Castro et al., 2014; Reinhardt & Bondy, 1994; Santi et al., 2018). Control mice received the same volume of 0.9% saline (i.p.). After that, five animals per group were processed for histology and five animals per group were sacrificed by decapitation and their brains were removed. The cortices were rapidly dissected on a cold plate, stored at  $-80^{\circ}\text{C}$ , and then processed to study gene expression by quantitative PCR (qPCR).

## 2.2 | Tissue fixation and immunohistochemistry

After treatments, animals were deeply anesthetized with pentobarbital (50 mg/kg body weight) and perfused through the left cardiac ventricle, first with pre-warmed ( $37^{\circ}\text{C}$ ) 0.9% NaCl and then for 5 min with 4% paraformaldehyde in 0.1 M phosphate buffer (pH 7.4;  $37^{\circ}\text{C}$ ). Brains were post-fixed for 4 h at  $4^{\circ}\text{C}$  in the same fixative and washed three times with 0.1 M phosphate buffer, pH 7.4 at room temperature. Coronal sections of the brain, 50  $\mu\text{m}$  thick, were obtained using a Vibratome (VT 1000S, Leica Microsystems, Wetzlar, Germany).

Immunohistochemistry was carried out in free-floating sections under moderate shaking. All washes and incubations were done in 0.1 M phosphate buffer pH 7.4, containing 0.3% bovine serum albumin and 0.3% Triton X-100. After several washes in buffer, sections were incubated overnight at  $4^{\circ}\text{C}$  with a rabbit antibody against glial fibrillary acidic protein (GFAP; diluted 1:1000; DAKO, USA), a marker of reactive astrocytes. Sections were then rinsed in buffer and incubated for 2 h at room temperature with a goat anti-rabbit Alexa secondary antibody (diluted 1:1000; 488 nm). Glass coverslip were mounted on slides with Vectashield antifade mounting medium with DAPI (Vector Laboratories, Burlingame, CA, USA). Whole cortex images were acquired with a Leica TCS-SP5 confocal system. Images analyzed were observed in a Leica DMI6000 fluorescent microscope equipped with a Leica DFC350 FX digital camera. From the cortex of each animal, at least four independent photographs were taken in the same cortex region of equivalent histological sections between animals. In each photo, a similar fluorescence detection threshold was applied to all photographs to reduce background noise and keep the signal corresponding to astrocytes. Later on, the entire area selected by the threshold was used as ROI and an investigator that was unaware of the identity of the experimental groups, measured the integrated density (product of the intensity of the GFAP signal by the area) to consider both the expression of GFAP (intensity signal) as well

as the size and spread of the astrocytes (area). Data were relativized to the values of the male control group.

## 2.3 | Cortical astrocyte cultures

Astrocytes were cultured from male and female P0–P2 pups, separately. Animals were sexed via measurement of anogenital distance, the brain was extracted, meninges were removed and the cerebral cortex was isolated under a dissecting microscope and then mechanically dissociated and washed twice in Hank's balanced salt solution (Sigma-Aldrich, Tres Cantos, Madrid). After complete dissociation in Dulbecco's modified Eagle's medium/Nutrient mixture F-12 (DMEM/F-12) culture medium with phenol red (Sigma-Aldrich) containing 10% fetal bovine serum (FBS, Invitrogen, Carlsbad, CA) and 1% antibiotic-antimycotic (Invitrogen), the cells were filtered through a 40- $\mu\text{m}$  nylon cell strainer (Corning Inc., Corning, NY). Cells were then centrifuged, resuspended in the same medium, and plated onto poly-L-lysine-coated 75- $\text{cm}^2$  flasks at  $37^{\circ}\text{C}$  and 5%  $\text{CO}_2$ . Medium was replaced after the first day in vitro and two times per week until the cells reached confluence ( $\sim 7$  days). Then, the cell cultures were shaken overnight at  $37^{\circ}\text{C}$  and 280 rpm on a tabletop shaker (Infors HT, Bottmingen, Switzerland) in order to minimize oligodendrocyte and microglia contamination. Astrocytes were incubated with 0.5% trypsin (Sigma-Aldrich), centrifuged, resuspended in phenol red-free DMEM/F-12 with 10% FBS and 1% antibiotic-antimycotic, and seeded in poly-L-lysine-coated 75- $\text{cm}^2$  flasks at  $37^{\circ}\text{C}$  and 5%  $\text{CO}_2$ . When cells reached confluence for the second time ( $\sim$ after 5 days), the subculture process was repeated but astrocytes were plated onto poly-L-lysine-coated plates (6, or 12 wells) at a density of 30,000 cells/ $\text{cm}^2$  or at a density of 10,000 cells/ $\text{cm}^2$  on poly-L-lysine-coated glass coverslips, using phenol red-free DMEM/F-12 with 10% FBS and 1% antibiotic-antimycotic. Twenty-four hours after plating, astrocytes were treated with vehicle, EGF (100 ng/ml, Sigma Aldrich) or LPS (1  $\mu\text{g}/\text{ml}$ , O26:B6, Sigma Aldrich) plus/or IGF-1 (100 nM, PeproTech) and three PI3K inhibitors, AG66 (#A8354, APExBIO, USA), TGX-221 (#A2681, APExBIO, USA) and CAL-101 (#A3005, APExBIO, USA), during 24 h. The concentrations used for the test compounds were chosen on the basis of previous studies (Bellini et al., 2011; Cerciat et al., 2010). After the incubation with the test compounds, astrocytes were processed for qRT-PCR, western blot, or phagocytosis experiments as indicated below.

## 2.4 | Quantitative real-time polymerase chain reaction (qRT-PCR)

Following experimental treatments, the cortices were homogenized in TRIzol reagent (Invitrogen, Carlsbad, CA, USA), and RNA extracted. In cell culture experiments, cells were harvested from six-well plates and total RNA was extracted using an Illustra RNAspin Mini kit (GE Healthcare, Madrid). First-strand cDNA was prepared from 0.75  $\mu\text{g}$  RNA using M-MLV reverse transcriptase (Promega,



Alcobendas, Madrid) according to the manufacturer's protocol. After reverse transcription, cDNAs were amplified by real-time PCR in 10  $\mu$ l reaction volume using SYBR Green Master Mix (Applied Biosystems, Foster City, CA) and the ABI Prism 7500 Sequence Detection System (Applied Biosystems) with conventional Applied Biosystems cycling parameters (40 cycles of changing temperatures, first at 95°C for 15 s and then 60°C for a minute). All the primer sequences were designed using Primer Express software (Applied Biosystems) and are shown in Table 1. For each primer pair, an appropriate dilution of cDNA was chosen in order to achieve the same amplification efficiency as that of the housekeeping genes (18S rRNA, Rpl13A, and GLAST). Changes in mRNA expression were calculated following the D<sub>C</sub>t method, using the Best Keeper index (Pfaffl et al., 2004) as total mRNA load reference for each sample.

## 2.5 | Co-immunoprecipitation

Immunoprecipitation experiments were performed in confluent primary astrocyte cultures. Cells were stimulated with IGF-1 during 45 min in order to activate the IGF-1R and promote the formation of IGF-1R/PI3K complex. After stimulation, the medium was removed and cells were lysated with Lysis Buffer (150 mM NaCl; GIBCO, 10 mM Tris pH 7.5; GIBCO, 1 mM EDTA; GIBCO, 1 mM EGTA; GIBCO, 1% Triton X-100; Sigma Aldrich, 0.5% NP-40; Roche, Protease Inhibitor Cocktail 0.01 mg/ml; Sigma Aldrich, 2 mM PMSF; Sigma Aldrich in dH<sub>2</sub>O). Lysates were centrifuged at 14,000 rpm for 15 min at 4°C. Supernatants were placed in clean tubes and were incubated with 10  $\mu$ l of anti-IGF-1-R primary antibody (Cell Signaling, #3027) or normal rabbit IgG. Samples were mixed in a rocking platform overnight at 4°C. Next day, 50  $\mu$ l of protein A agarose (Invitrogen, 15918-014) were added to each tube and mixed in a rocking platform at 4°C for 1 h. Then, samples were centrifuged at 14,000 rpm at 4°C for 2 min. Supernatants were removed and the pellets were washed 3 times with lysis buffer diluted 1/2. Finally, the pellets were resuspended in 50  $\mu$ l of 2 $\times$  Laemmli buffer. Samples were boiled for 3 min and spun at 14,000 rpm for 2 min. Supernatants were used for western blots assay.

**TABLE 1** Primer sequence for quantitative PCR

Gene	Forward (5'-3')	Reverse (5'-3')
18S rRNA	CGCCGCTAGAGGTGAAATTCT	CATTCTTGGCAAATGCTTTCG
Rpl13A	TCACCAGAAAGTTTGCTTACCTGGG	TGCCTGTTTCCGTAACCTCAAG
GFAP	GGTCCGCTTCTGGAACA	GCTCCGCTGGTAGACATCA
GLAST	CGCGGTGATAATGTGGTATGC	GGCAAGCTGTCCCCCAAT
IL-1 $\beta$	CGACAAAATACCTGTGGCCT	TTCTTTGGGTATTGCTTGGG
IL-6	GAAACCGCTATGAAGTTCCTCTCTG	TGTTGGGAGTGGTATCCTCTGTGA
IL-10	CTGGCTCAGCACTGCTATGCT	ACTGGGAAGTGGGTGCAGTT
iNOS	CGTACCGGATGAGCTGTGAA	GCCACCAACAATGGCAACA
IP-10	CAGTGAGAATGAGGGCCATAGG	CGGATTCAGACATCTCTGCTCAT
TLR2	TGTCCGCAATCATAGTTTCTGATG	AGCAGAGAAGTGAAGCCCT
TLR4	GGCTCCTGGCTAGGACTCTGA	TCTGATCCATGCATTGGTAGTT

## 2.6 | Western blotting

After the experimental treatments, cells were lysed and solubilized in 200  $\mu$ l of Laemmli loading buffer. Samples were boiled and sonicated for 5 min. Solubilized proteins (20  $\mu$ l) were resolved by 8% and 10% SDS-PAGE and then electrophoretically transferred to 0.2  $\mu$ m Trans-Blot Turbo nitrocellulose membranes (BioRad, Alcobendas, Madrid). The membranes were blocked at room temperature for 90 min in Tris-buffered saline containing 0.1% Tween 20 and 5% BSA. Then, the membranes were incubated overnight at 4°C with primary antibodies diluted in the same blocking solution. After that, the membranes were incubated with infrared dye-conjugated antibodies (diluted 1:10,000; LI-COR Biosciences, Lincoln, NE). Specific proteins were visualized by Odyssey Infrared Imaging System (LI-COR Biosciences). The following primary antibodies were used: anti-AKT (diluted 1:1000; SC-8312, Santa Cruz), anti-p-AKT (diluted 1:1000; #9271, Cell Signaling), anti-IGF-1R (diluted 1:1000; #3027, Cell Signaling), anti-p110 $\alpha$  (diluted 1:1000; C73F8, Cell Signaling), anti-p110 $\beta$  (diluted 1:1000; C33D4, Cell Signaling), anti-p110 $\delta$  (diluted 1:1000; D1Q7R, Cell Signaling) and anti- $\alpha$ -tubulin (diluted 1:5000; #T5168, Sigma-Aldrich). Data were normalized to the  $\alpha$ -tubulin expression.

## 2.7 | Preparation of Cy3 conjugated brain-derived cellular debris

Cellular debris was obtained from male and female mouse embryonic day 17 hippocampi. The hippocampi were dissected out and dissociated to single cells after digestion for 15 min with 0.5% of trypsin (Worthington Biochemicals, Freehold, NJ) and DNase I (Sigma-Aldrich). Cells were then centrifuged at 280 g for 5 min and the pellet was resuspended in 1 ml of Neurobasal culture medium (Invitrogen, ThermoFisher Scientific). Cell suspension was sonicated at 20 kHz for 2 s and the cellular debris were labeled using Cy<sup>3</sup> (Mono-Reactive Dye Pack; Amersham Biosciences, VWR, Radnor, PA) according to the manufacturer's instructions. Cy3 conjugated cellular debris was stored at 4°C until their use.



## 2.8 | Phagocytosis assays

The phagocytosis activity of primary astrocytes was assessed using brain-derived cellular debris to mimic phagocytosis activated by neural cell signals. Thus, male and female astrocyte cultures were incubated for 1 h at 37°C with mouse Cy3-conjugated brain-derived cellular debris (10 µl/ml) obtained from male and female hippocampi, respectively. As negative control group, astrocyte culture was placed on ice and then the pre-cooled cell debris was added and incubated on ice for 1 h. Next, astrocyte cultures were washed twice with phosphate-buffered saline (PBS) and fixed for 20 min at room temperature with 4% paraformaldehyde in PBS. After several washes with PBS-gelatin and permeabilized with PBS-triton x-100, astrocyte cultures were incubated with rabbit GFAP protein antibody (diluted 1:1000; DAKO, Agilent, Santa Clara, CA), followed by incubation with a goat anti-rabbit Alexa488-conjugated secondary antibody (1:1000; Jackson Immuno-Research Europe Ltd., Ely, Cambridge-shire). After washing with PBS, glass coverslips were mounted on slides with Vectashield antifade mounting medium containing DAPI (Vector Laboratories, Burlingame, CA). Cell cultures were observed in a Leica DMI6000 fluorescent microscope equipped with a Leica DFC350 FX digital camera and with a Leica TCS SP5 direct confocal microscope.

## 2.9 | Image analysis

Internalization of cellular debris within the cytoplasm of GFAP immunoreactive cells was confirmed by assessing Cy3 dye-emitted fluorescence, in Z-stack images that were visualized on a Leica TCS-SP5 confocal system. Then, image analysis of the astrocyte cultures was performed on microphotographs obtained on a Leica DMI6000 fluorescent microscope using a × 20 objective and a Leica DFC350 FX digital camera. All microphotographs for quantitative analysis were taken with the same intensity and exposure. Fluorescence intensity was assessed using the Fiji imaging-processing package (ImageJ 1.52n, National Institutes of Health, USA). The amount of cellular internalization of Cy3-conjugated cellular debris was quantified by measuring the intensity of Cy3 dye-emitted fluorescence in a given GFAP immunoreactive area. Cell images were obtained from at least four independent cultures for each experimental group. Ten random images were obtained for each culture and experimental condition and between 150 and 1000 cells were analyzed per experimental group.

## 2.10 | Statistical analysis

Data shown in the figures are presented as the mean ± standard error of the mean (SEM). The size of the experimental groups corresponds to the number of animals or independent culture preparations, and it is indicated in each figure legend. However, in the

phagocytosis experiments, the data are presented as median ± ranges, since the values obtained in the phagocytosis assays did not follow a normal distribution. The ranges included the highest and lowest values of intensity and the n for statistical analysis was the number of cells ( $n = 150$ –1000 cells per experimental group). Statistical analyses were carried out using GraphPad Prism software version 8.0 for Windows. Normality of the data was assessed with the Kolmogorov–Smirnov test, to satisfy the assumption of normality for the analysis of variance (ANOVA). Differences between two experimental groups were analyzed by Student's *t* test. Interactions between sex and treatment was determined using the two-way ANOVA interaction model, with Tukey's post hoc multiple comparisons or Fisher's exact test to analyze differences between percentage of GFAP expression. Whenever normality was not achieved, statistical significance was determined with nonparametric tests (Kruskal–Wallis and post hoc pairwise comparisons with Dunn's test). Differences between two experimental groups were analyzed by Mann–Whitney *U* test. The statistical significance level was set at  $p < .05$  in all cases.

## 3 | RESULTS

### 3.1 | IGF-1 modulates, in a sex-dependent manner, mouse cortex astrogliosis caused by systemic application of LPS

It is widely known that the intraperitoneal administration of LPS is a model of mild neuroinflammation and several studies showed anti-inflammatory effects of IGF-1 acting on astrocytes and microglia in this model, counteracting the expression of the inflammatory marker glial fibrillary acidic protein (GFAP) (Labandeira-Garcia et al., 2017; Park et al., 2011). To assess whether these effects are sexually dimorphic, GFAP expression was evaluated by fluorescence immunohistochemistry and integrated density quantification in the cortex of male and female mice treated with LPS and IGF-1 (Figure 1b). Two-way ANOVA revealed an effect of treatment without interaction between sex and treatment ( $F[2, 110] = 6.946$ ;  $p = .0014$ ) and Uncorrected Fisher's LSD test showed that LPS provoked a significant increase of GFAP in male and female cortex ( $p = .0034$  and  $p = .0327$ , respectively). However, IGF-1 treatment was able to decrease these levels in males ( $p = .0272$  vs. LPS treatment), with no significant effect over females (Figure 1c). In agreement with the results from immunohistochemistry, two-way ANOVA analysis of the GFAP mRNA expression in the mouse cortex showed significant effects of sex ( $F[1, 24] = 13.24$ ;  $p = .0013$ ) and treatment ( $F[2, 24] = 11.33$ ;  $p = .0003$ ) without interaction. Tukey's test indicated that GFAP mRNA expression was significantly increased in both sexes after treatment with LPS ( $p = .0087$  and  $p = .0161$ , respectively) and that the LPS effect was impaired by IGF-1 in male and not in female animals ( $p = .3944$  and  $.0018$ , respectively, vs. vehicle treated mice). These sexual differences led us to evaluate the cellular and molecular

changes produced in astrocytes in this experimental paradigm using primary astrocyte cultures.

### 3.2 | Male and female astrocytes show different inflammatory outcomes with LPS administration and IGF-1 treatment

Previously we demonstrated that LPS induces a reactive inflammatory phenotype in primary astrocytes (Acas-Fonseca et al., 2019). To evaluate if this astrocytic response is sexually dimorphic and also the effect of IGF-1 treatment, primary astrocyte cultures from male and female mice were treated for 24 h with LPS and the expression levels of different inflammation-related genes were measured using RT-qPCR. As expected, LPS significantly increased mRNA levels of Toll-like receptor (TLR) 2 and 4 in both males and females when compared with control group. These changes were accompanied by an increase in mRNA expression of proinflammatory factors: inducible NO synthase (iNOS), chemokine interferon- $\gamma$ -inducible protein-10 (IP-10) (also named CXCL10), and cytokines (IL-1 $\beta$ , IL-6, and IL-10) both in male and female (Figure 2 and Table 2). IGF-1 did not produce any effect in control conditions but was able to counteract the effect of LPS on mRNA levels of TLR4 but not of TLR2, iNOS, and IP10 in both sexes; two way ANOVA analysis with Tukey's corrections indicated that IGF-1 counteracted the effect of LPS on cytokines mRNA expression in male but not in female and showed an effect of sex and treatment without interaction in the expression of iNOS, IL-6, and IL-10 (Figure 2 and

Table 2). In summary, these results indicate that male and female astrocytes respond differently to an inflammatory stimulus and to the treatment with IGF-1.

### 3.3 | Phagocytosis of reactive astrocytes is modulated by IGF-1 only in male astrocytes

We previously reported that LPS significantly stimulated neural debris phagocytosis in male astrocytes while exerted a reduction in females (Crespo-Castrillo et al., 2020). Since our present results indicated that IGF-1 counteracts certain aspects of the astrocyte inflammatory response to LPS in males, we assessed whether IGF-1 was also able to modulate the changes induced by LPS on astrocyte phagocytosis. Astrocytes were treated with LPS and/or IGF-1 for 24 h. In resting conditions phagocytosis of female astrocytes was greater than that of male (Mann Whitney test,  $p = .0064$ ). As we previously showed, Kruskal-Wallis followed by Dunn's multiple comparisons test indicated that LPS treatment significantly stimulated Cy3 labeling in male astrocytes, compared to basal conditions ( $p = .0359$ ) while exerted a significant inhibitory effect on Cy3 labeling of female astrocytes ( $p < .0001$ ) (Figure 3). IGF-1 treatment did not produce any effect on astrocyte phagocytosis of both sexes; however, IGF-1 was able to counteract the effect of LPS on phagocytosis in male astrocytes ( $p < .0001$ ) but not in females ( $p = .8101$ ) (Figure 3). These results indicate that IGF-1 affects LPS-stimulated astrocyte phagocytosis in male and female mice in a different way.

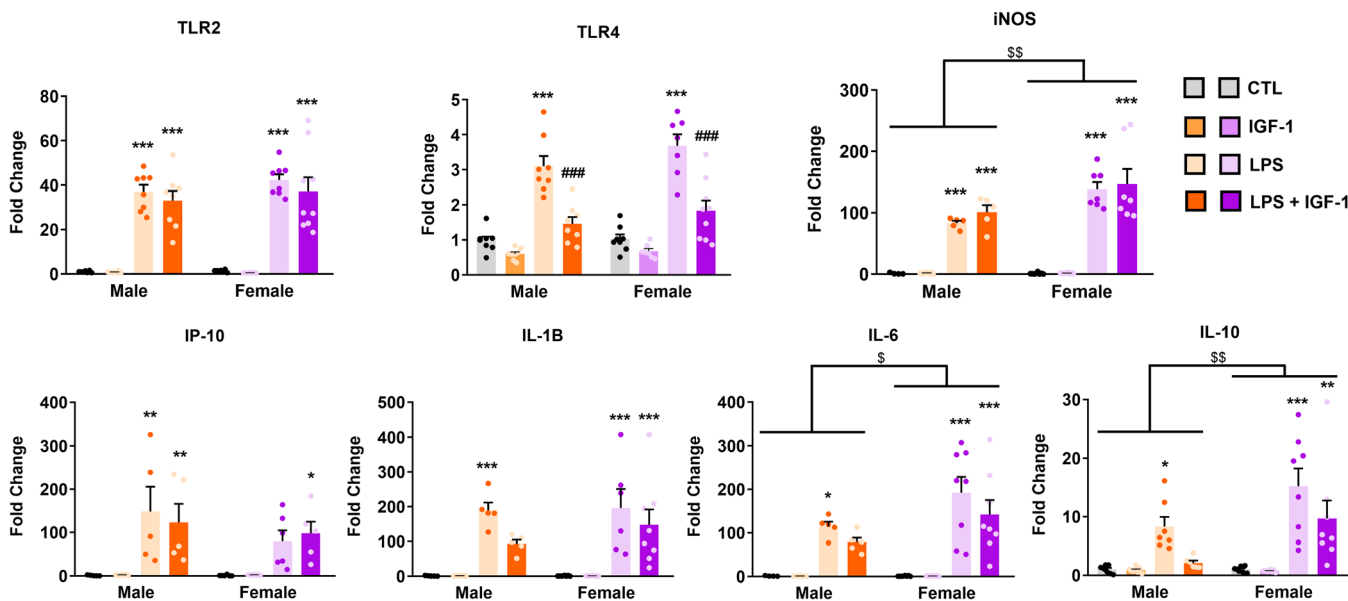


**FIGURE 2** Effect of IGF-1 on the LPS-induced inflammatory response in primary astrocytes from male and female mouse cortex. Astrocyte cultures were incubated for 24 h with 1  $\mu$ g/ml LPS and/or 100 nM IGF-1. The mRNA levels of TLR4, TLR2, iNOS, IP-10, IL-1 $\beta$ , IL-6, and IL-10 were measured on cell lysates by qRT-PCR. The graphs show mRNA levels in cultures treated with vehicles (control), LPS, or LPS plus IGF-1. Data represent the mean  $\pm$  SEM. \* $p < .05$ ; \*\* $p < .01$ ; \*\*\* $p < .001$  effect of treatment in male and female astrocytes versus control groups and ### $p < .001$  versus LPS treated groups, measured by 2-way ANOVA followed by Tukey's multiple comparisons post hoc test. \$ $p < .05$ ; \$\$ $p < .01$  sex differences



**TABLE 2** Effects of LPS and IGF-1 on inflammatory gene expression of male and female mouse astrocytes

Gene	Sex	Gene fold changes															
		2-way ANOVA					Male					Female					
		Treatment	Interaction sex*treatment	Control	IGF-1	LPS	Control	IGF-1	LPS	LPS + IGF-1	Control	IGF-1	LPS	LPS + IGF-1	Control	IGF-1	LPS
TLR2	$F(1, 53) = 0.96$	$p = .3298$	$F(3, 53) = 76.68$	$p < .0001$	$1.00 \pm 0.14$	$0.78 \pm 0.12$	$37.12 \pm 3.01$	$33.01 \pm 4.38$	$1.33 \pm 0.19$	$0.49 \pm 0.04$	$42.29 \pm 2.51$	$37.30 \pm 6.17$	$1.83 \pm 0.29$	$1.03 \pm 0.13$	$0.68 \pm 0.07$	$3.68 \pm 0.32$	$1.83 \pm 0.29$
TLR4	$F(1, 55) = 3.34$	$p = .0730$	$F(3, 55) = 64.23$	$p < .0001$	$0.98 \pm 0.11$	$0.60 \pm 0.06$	$3.10 \pm 0.29$	$1.46 \pm 0.19$	$1.03 \pm 0.13$	$0.68 \pm 0.07$	$3.68 \pm 0.32$	$1.83 \pm 0.29$	$1.03 \pm 0.13$	$0.68 \pm 0.07$	$3.68 \pm 0.32$	$1.83 \pm 0.29$	$1.83 \pm 0.29$
iNOS	$F(1, 44) = 10.02$	$p = .0028$	$F(3, 44) = 72.66$	$p < .0001$	$1.00 \pm 0.60$	$1.56 \pm 0.27$	$83.19 \pm 3.81$	$100.98 \pm 11.60$	$0.98 \pm 0.48$	$1.52 \pm 0.22$	$138.20 \pm 11.61$	$147.71 \pm 24.55$	$1.83 \pm 0.29$	$0.98 \pm 0.48$	$1.52 \pm 0.22$	$138.20 \pm 11.61$	$147.71 \pm 24.55$
IP-10	$F(1, 41) = 1.94$	$p = .1703$	$F(3, 41) = 14.61$	$p < .0001$	$1.00 \pm 0.46$	$2.05 \pm 0.31$	$148.35 \pm 57.20$	$122.93 \pm 43.14$	$1.04 \pm 0.57$	$2.22 \pm 0.18$	$79.33 \pm 25.06$	$97.60 \pm 27.22$	$1.83 \pm 0.29$	$1.04 \pm 0.57$	$2.22 \pm 0.18$	$79.33 \pm 25.06$	$97.60 \pm 27.22$
IL-1 $\beta$	$F(1, 45) = 0.66$	$p = .4209$	$F(3, 45) = 24.11$	$p < .0001$	$1.00 \pm 0.39$	$1.20 \pm 0.31$	$189.45 \pm 22.42$	$93.01 \pm 11.77$	$1.02 \pm 0.34$	$0.96 \pm 0.22$	$196.44 \pm 53.80$	$148.10 \pm 43.55$	$1.83 \pm 0.29$	$1.02 \pm 0.34$	$0.96 \pm 0.22$	$196.44 \pm 53.80$	$148.10 \pm 43.55$
IL-6	$F(1, 46) = 5.13$	$p = .0282$	$F(3, 46) = 25.32$	$p < .0001$	$1.00 \pm 0.43$	$0.94 \pm 0.14$	$114.74 \pm 10.69$	$78.43 \pm 10.38$	$1.08 \pm 0.32$	$1.04 \pm 0.23$	$191.93 \pm 36.41$	$142.013 \pm 32.95$	$1.83 \pm 0.29$	$1.08 \pm 0.32$	$1.04 \pm 0.23$	$191.93 \pm 36.41$	$142.013 \pm 32.95$
IL-10	$F(1, 51) = 8.10$	$p = .0063$	$F(3, 51) = 17.37$	$p < .0001$	$1.00 \pm 0.25$	$0.90 \pm 0.16$	$8.32 \pm 1.63$	$2.11 \pm 0.40$	$1.01 \pm 0.19$	$0.73 \pm 0.06$	$15.21 \pm 3.03$	$9.67 \pm 3.09$	$1.83 \pm 0.29$	$1.01 \pm 0.19$	$0.73 \pm 0.06$	$15.21 \pm 3.03$	$9.67 \pm 3.09$

Note: Table shows how treatments (IGF-1, LPS, or LPS + IGF-1) affects gene expression in male and female astrocytes. The average of the male control group was considered the control mean value. Each individual sample's fold change was compared to the control mean. Fold changes are presented in table as mean values of all samples in each group  $\pm$  SEM. Statistical significance analysis was assessed by using two-way ANOVA, followed by Tukey's multiple comparisons post hoc test. A value of  $p < .05$  was considered significant, in bold: statistically significant.



### 3.4 | IGF-1 is able to stimulate astrocytic AKT phosphorylation in a sex-specific manner

Next, we sought to determine the molecular mechanism by which IGF-1 regulates neuroinflammation and phagocytosis in astrocytes. Previous studies have shown that IGF-1 activates PI3K signaling in the nervous system through the IGF-1 receptor (IGF-1R) by interacting with estrogen receptors ERalpha (Garcia-Segura et al., 2010; Mendez et al., 2003)

and GPER (Yuan et al., 2021). These findings indicate a possible sex-dimorphism in IGF-1 actions that have not been explored. Therefore, we analyzed: i) the activity of PI3K in primary astrocytes of both sexes treated with LPS and IGF-1 by measuring the level of phosphorylation of AKT (p-AKT) and ii) which catalytic isoform of PI3K is involved in the activation of the PI3K / AKT pathway by IGF-1 in astrocytes.

Surprisingly, the basal levels of p-AKT were higher in female astrocytes compared to the male (unpaired *t* test,  $p = .0145$ )

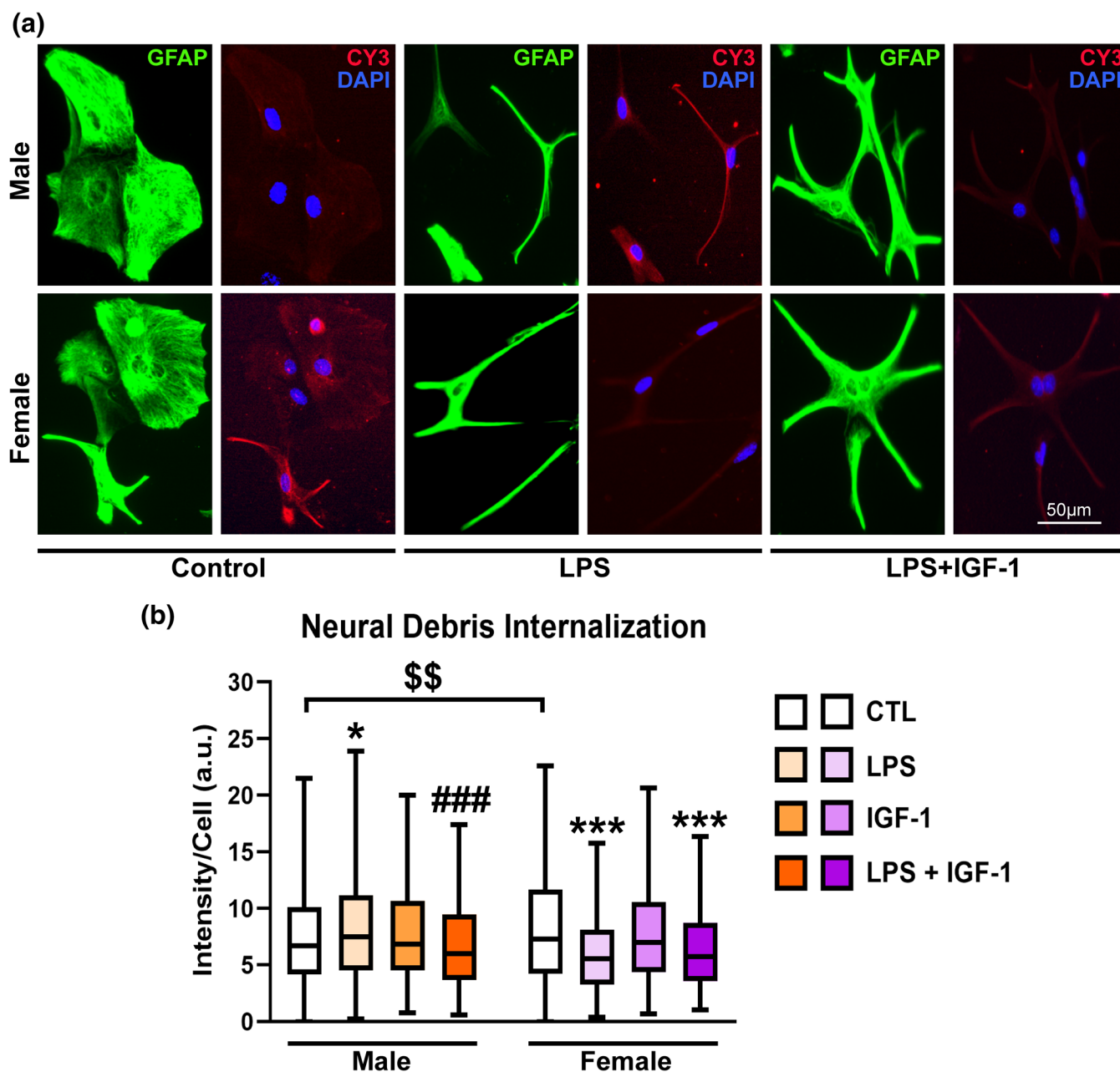


**FIGURE 3** IGF-1 modulates phagocytosis of reactive male astrocytes. (a) Representative images of male and female astrocyte cultures treated for 24 h with vehicle, LPS and IGF-1 and then incubated for 1 h with Cy3 conjugated brain-derived cellular debris (red). Cells were immunostained for GFAP (green) and cell nuclei were stained with DAPI. (b) Cy3 fluorescence intensity per cell in male and female astrocytes. Data are presented as median  $\pm$  ranges. Significant differences  $*p < .05$ ;  $***p < .001$ , effect of treatment versus the control group of the same sex and  $###p < .001$  versus LPS treated groups, measured by the Kruskal-Wallis test, followed by Dunn's multiple comparisons post hoc test,  $$$$p < .001$  basal sex differences measured by Mann-Whitney *U* test.  $N = 4-8$  independent cultures

(Figure 4a). When pAKT level was evaluated in astrocytes treated with LPS and/or IGF-1, two-way ANOVA followed by Tukey's multiple comparisons test, showed an effect of treatment ( $F[3, 36] = 20.32$ ;  $p < .0001$ ) with interaction between sex and treatment ( $F[3, 36] = 6.302$ ;  $p = .0015$ ). Treatment with LPS had no significant effect on the level of p-AKT neither in males or females. However, IGF-1 was able to increase p-AKT in male astrocytes both in resting and inflammatory conditions ( $p = .0002$  and  $p < .0001$ , respectively). However, in female astrocytes IGF-1 did not have any significant effect neither under resting nor inflammatory conditions (Figure 4a). Since PI3K and AKT are expressed both in males and females, we treated astrocytes with another neurotrophic factor to check the capability to enhance AKT phosphorylation in females. Figure 4b shows that EGF, unlike IGF-1, induces a significant increase of pAKT in males (unpaired *t* test,  $p = .0038$ ) and also in females ( $p = .0158$ ). It has been described that activation of IGF-1R provokes the formation of a multimolecular complex made up of ERs, IGF-1R and components of the IGF-1R signaling pathway, such as insulin receptor substrate 1 (IRS1), PI3K (constituted by p85 and p110 subunits), and AKT

(Arevalo et al., 2015). Taking advantage of PI3K inhibitors, AG66, TGX-221, and CAL-101, with selectivity toward p110 catalytic isoforms p110 $\alpha$ , p110 $\beta$ , and p110 $\delta$  respectively, we assessed if sex differences observed with IGF-1 treatment were due to different PI3K catalytic isoforms involved. The actions of the inhibitors on the pAKT/AKT ratio in astrocytes treated with LPS + IGF-1 were analyzed by two-way ANOVA followed by Tukey's multiple comparisons test, showing a treatment effect ( $F[3, 33] = 6.252$ ;  $p = .0018$ ) with interaction between sex and treatment ( $F[3, 33] = 3518$ ;  $p = .0257$ ). The three inhibitors tested were able to significantly reduce pAKT level compared with LPS + IGF group in male astrocytes ( $p = .0008$  for AG66;  $p = .0094$  for TGX-221;  $p = .0005$  for CAL-101). However, no effect was observed in the case of female astrocytes with any of the inhibitors tested. This suggests that all isoforms of p110 are involved in the increased IGF-1-induced phosphorylation of AKT in males.

As results showed sex variability in PI3K-AKT pathway, we next wanted to evaluate if functional differences observed with IGF-1 treatment were due to different PI3K catalytic isoforms implicated.

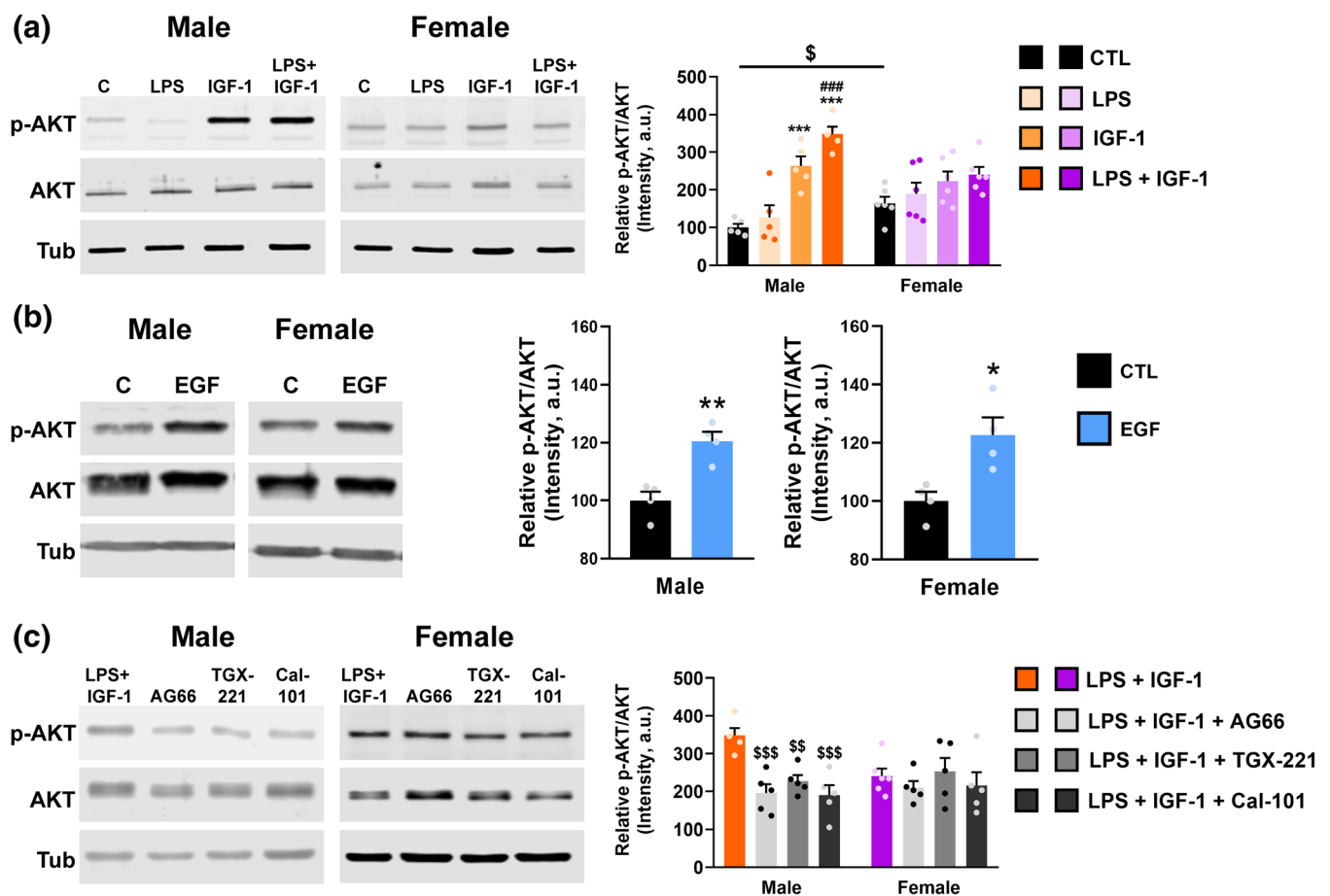


**FIGURE 4** Sex differences in AKT phosphorylation in astrocytes. Primary cultures of male and female astrocytes were treated for 24 h. with vehicle, LPS and/or IGF-1 (a), EGF (b) and three PI3K isoform-specific inhibitors, AG66, TGX-221E, and CAL-101 (c) and the level of AKT phosphorylation was evaluated by western blot using  $\alpha$ -tubulin as a loading control. Graphs represent quantitative analysis of pAKT/AKT expressed as mean  $\pm$  SEM. Significant differences  $***p < .001$ , effect of treatment versus control groups,  $###p < .001$  versus LPS treated groups and  $$$$p < .01$ ;  $$$$$p < .001$  versus LPS + IGF-1, measured by 2-way ANOVA followed by Tukey's multiple comparisons post hoc test in (a) and (c) and by unpaired two-tailed *t* test in (b).  $N = 4$ –5 independent cultures

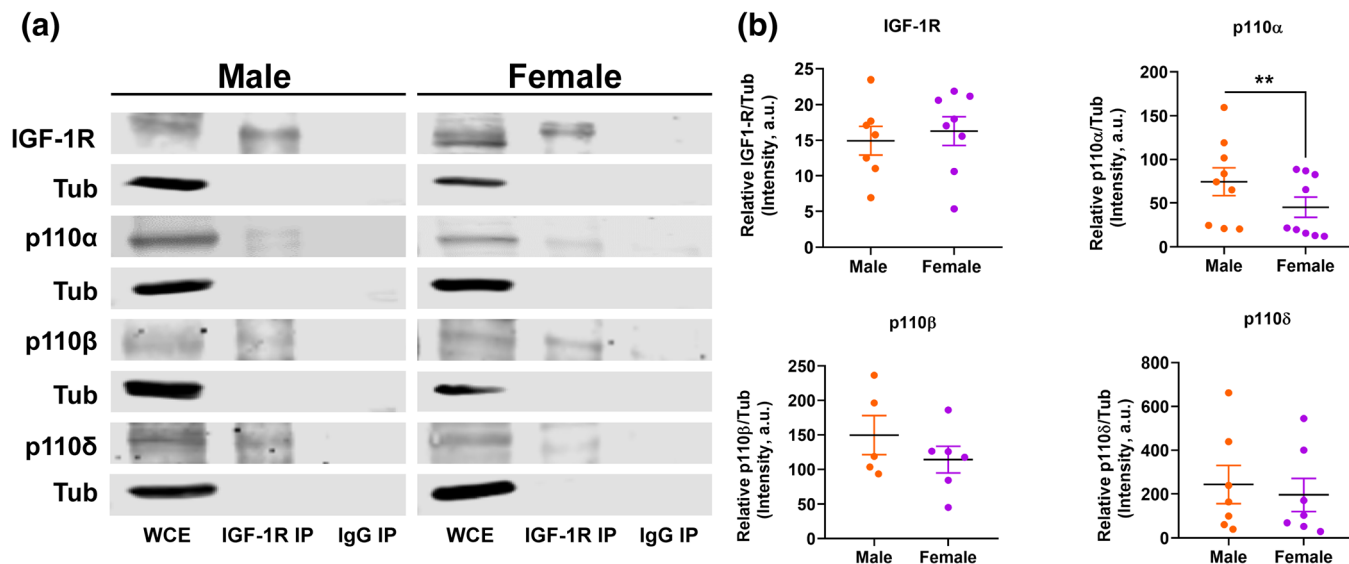


**FIGURE 5** The three catalytic subunits of PI3K immunoprecipitate with IGF-1R in male and females but have different expression levels between sexes. Primary astrocyte cultures were stimulated with IGF-1 during 45 min in order to activate the IGF-1R and promote the formation of IGF-1R/PI3K complex. Cell lysates were immunoprecipitated with IGF-1-R antibody or normal rabbit IgG and then immunoblotted with the indicated antibodies.  $N = 5-9$  independent cultures. (a) Representative image showing lane 1—IGF-1R co-IP positive control, lanes 3, 5 y 7—p110 $\alpha$ ,  $\beta$ , and  $\delta$  co-elutes with IGF-1R. WCE, whole-cell extract, IGF-1R-IP, IGF-1R co-immunoprecipitation. (b) Quantitative analysis of the p110 $\alpha$ ,  $\beta$ , and  $\delta$  and IGF-1R expression levels evaluated in the whole-cell extract of male and female astrocytes. Data are presented as means  $\pm$  SEM, \*\* $p < .01$  indicates basal sex differences measured by unpaired two-tailed  $t$  test

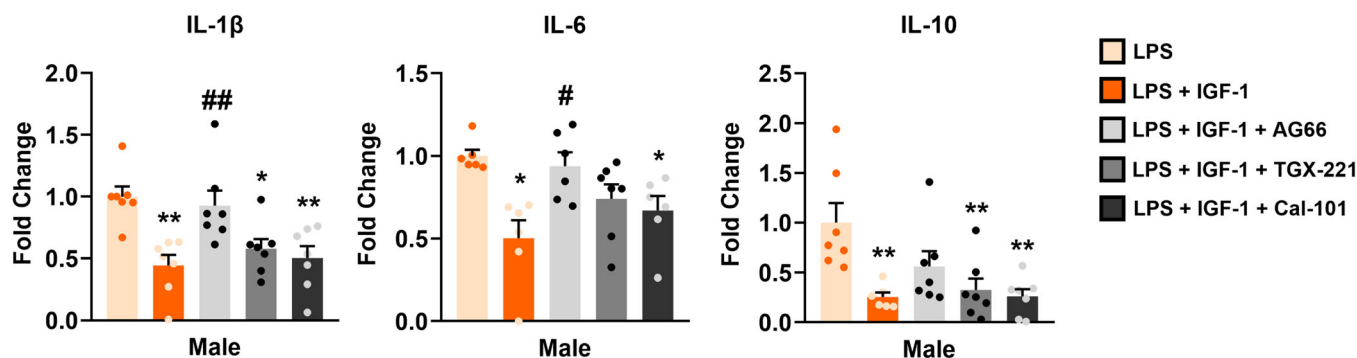


**FIGURE 6** Effect of selective inhibitors of PI3K isoforms on IGF-1 modulation of male astrocytic inflammatory response. PI3K pathway was blocked with isoform-selective PI3K inhibitors in astrocytes treated with LPS + IGF-1. Graphs show the expression of IL-1 $\beta$ , IL-6, and IL-10 mRNA quantified by q-RT-PCR. Note that only the p110 $\alpha$  inhibitor AG66 significantly suppressed the IGF-1 effect on the IL-6 and IL-10 mRNA expression in male astrocytes, whereas TGX-221 and CAL-101 had no effect, suggesting that p110 $\alpha$  subunit drives IGF-1 modulation of astrocytic inflammatory response. Data are presented as means  $\pm$  SEM. Significant differences \*\* $p < .01$ , effect of inhibitors versus LPS and # $p < .05$ , ## $p < .01$  versus LPS + IGF-1 treated groups, measured by ordinary one-way ANOVA followed by Tukey's multiple comparisons post hoc test.  $N = 6$  independent cultures

**TABLE 3** Effect of selective inhibitors of PI3K isoforms on IGF-1 modulation of inflammatory gene expression in reactive male astrocytes

Gene	One-way ANOVA Treatment	Gene fold changes				
		LPS	LPS + IGF1	LPS + IGF1 + AG66	LPS + IGF1 + TGX-221	LPS + IGF1 + CAL-101
IL-1 $\beta$	$F(4, 30) = 7.32 p = .0003$	1.00 $\pm$ 0.08	<b>0.44 <math>\pm</math> 0.09</b>	0.93 $\pm$ 0.12	<b>0.58 <math>\pm</math> 0.08</b>	<b>0.50 <math>\pm</math> 0.10</b>
IL-6	$F(4, 25) = 4.81 p = .0051$	1.05 $\pm$ 0.04	<b>0.63 <math>\pm</math> 0.06</b>	0.99 $\pm$ 0.09	0.78 $\pm$ 0.09	<b>0.70 <math>\pm</math> 0.09</b>
IL-10	$F(4, 29) = 5.76 p = .0015$	1.00 $\pm$ 0.19	<b>0.25 <math>\pm</math> 0.05</b>	0.56 $\pm$ 0.15	<b>0.32 <math>\pm</math> 0.11</b>	<b>0.26 <math>\pm</math> 0.07</b>

Note: Table shows how treatments affects gene expression in male astrocytes. The average of the astrocytes treated with LPS group was considered the control mean value. Each individual sample's fold change was compared to the control mean. Fold changes are presented in table as mean values of all samples in each group  $\pm$  SEM. Statistical significance analysis was assessed by using one-way ANOVA, followed by Tukey's multiple comparisons post hoc test. A value of  $p < .05$  was considered significant, In bold: statistically significant.

### 3.5 | Catalytic subunits of PI3K have different expression levels between sexes

Since the use of selective inhibitors revealed different outcomes in both sexes, we wanted to get further insight into the role of PI3K/p110 isoforms in the IGF-1 signaling pathway. For this, we evaluated

if p110 isoforms immunoprecipitated with IGF-1R. Data shown in Figure 5a demonstrates that in both sexes, all isoforms interact physically with IGF-1R. Nevertheless, we noticed that the expression of p110 $\alpha$ ,  $\beta$ , and  $\delta$  is higher in male astrocytes than in females, although the difference is significant only for p110 $\alpha$  ( $p = .0078$ ). In contrast, the expression of IGF-1R is similar in males and females (Figure 5b).

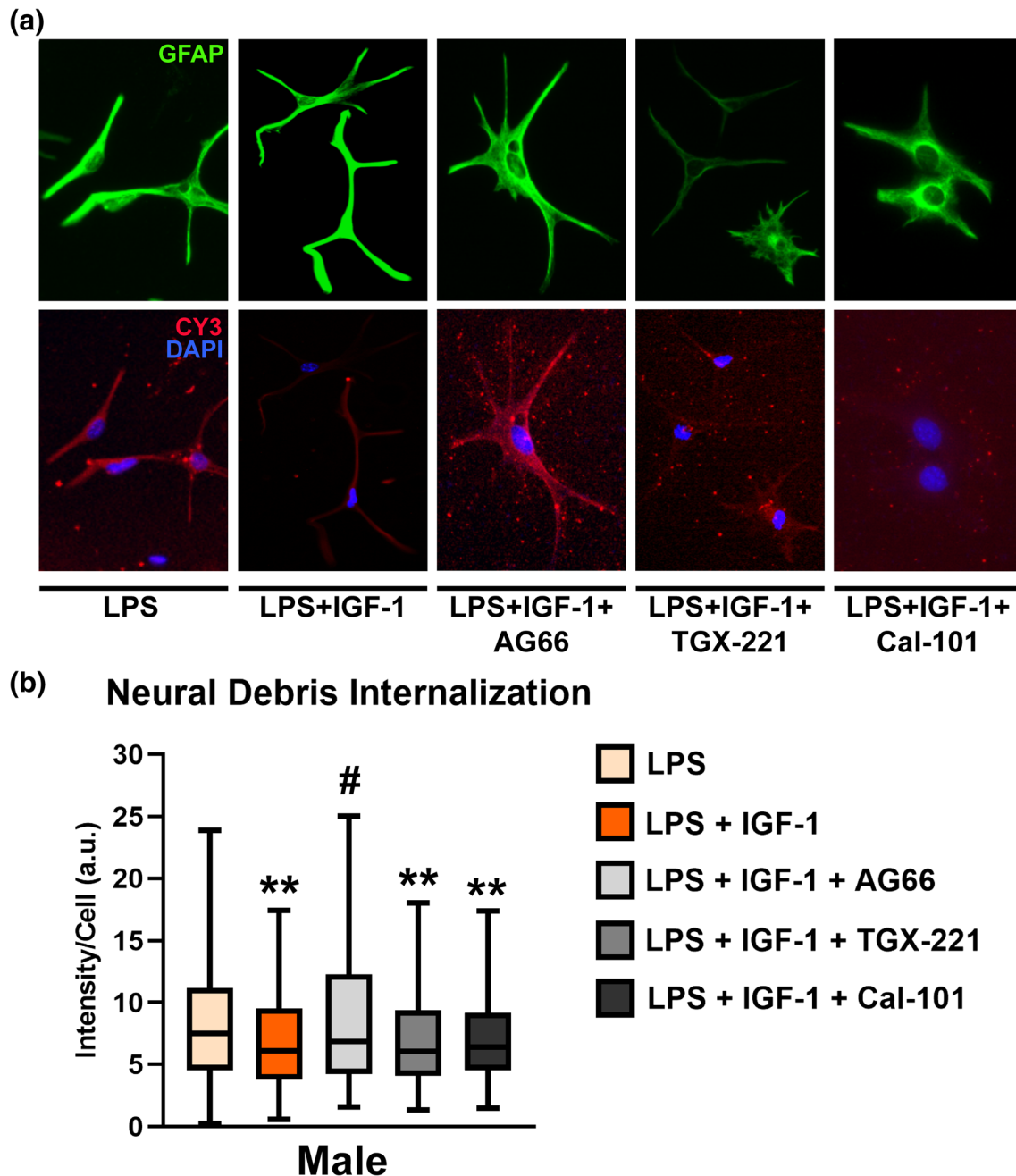


**FIGURE 7** Effect of selective inhibitors of PI3K isoforms on IGF-1 modulation of the male astrocytic phagocytosis. PI3K pathway was blocked with isoform-selective PI3K inhibitors in astrocytes treated with LPS + IGF-1. (a) Representative images of male astrocyte cultures incubated for 1 h with Cy3 conjugated brain-derived cellular debris (red) and immunostained for GFAP (green). Cell nuclei were stained with DAPI. (b) Graph shows Cy3 fluorescence intensity per cell. Only the p110 $\alpha$  inhibitor AG66 significantly suppressed the IGF-1 effect on the astrocyte phagocytosis, whereas TGX-221 and CAL-101 had no effect, suggesting that p110 $\alpha$  subunit drives IGF-1 modulation of astrocytic phagocytosis. Data are presented as median  $\pm$  ranges. Significant differences \*\* $p < .01$ , effect of inhibitors versus LPS and # $p < .05$  versus LPS + IGF-1 treated groups, measured by Kruskal-Wallis test followed by Dunn's multiple comparisons post hoc test.  $N = 4$  independent cultures



Together, these results suggest that sex-differences observed in the phosphorylation of AKT promoted by IGF-1, could be due to a lower expression of the catalytic subunits of PI3K in females, especially p110 $\alpha$ .

### 3.6 | IGF-1 modulates astrocytic inflammatory response through PI3K catalytic subunit p110 $\alpha$

Based on the above results, we wondered if PI3K is involved in the regulation of inflammation exerted by IGF-1 in primary astrocytes. To test this, we blocked the PI3K pathway with isoform-selective PI3K inhibitors in male astrocytes treated with LPS + IGF-1. Then, we analyzed the expression of IL-1 $\beta$ , IL-6, and IL-10 mRNA by q-RT-PCR. Figure 6 shows that only p110 $\alpha$  inhibitor AG66 significantly suppressed the IGF-1 effect on the IL-1 $\beta$ , IL-6, and IL-10 mRNA expression in males, whereas TGX-221 and CAL-101 had no effect (Figure 6 and Table 3). These results suggest that p110 $\alpha$  subunit drives IGF-1 modulation of male astrocytic inflammation.

### 3.7 | IGF-1 effect in male astrocytic phagocytosis is also regulated by p110 $\alpha$

Next, we assessed whether the PI3K pathway is also involved in the actions of IGF-1 on the phagocytic ability of male astrocytes stimulated with LPS. Figure 7 show that only the p110 $\alpha$  inhibitor AG66, was able to block the IGF-1 effect on debris engulfment by reactive astrocytes (Kruskal-Wallis followed by Dunn's multiple comparisons test,  $p = .01149$ ). On the contrary, TGX-221 and CAL-101 had no effect in phagocytosis. Results here indicate that p110 $\alpha$  subunit also regulates changes induced by IGF-1 in reactive male astrocyte phagocytosis.

## 4 | DISCUSSION

The present study analyzes the effects of exogenous IGF-1 on neuroinflammation and phagocytosis of reactive astrocytes. Using male and female mice we have found that systemic administration of LPS produces an increase of GFAP expression in cortical astrocytes, which agrees with previous studies (W. Li et al., 2021). In addition, co-treatment with IGF-1 returns GFAP expression to basal levels in males without any effect in female. These results prompted us to explore the molecular and cellular processes that lead to such sex differences. To do that we used astrocyte primary cultures derived from the cerebral cortices of neonatal male and female mice that were treated with LPS and IGF-1. In this model our results showed that LPS significantly upregulated astrocyte mRNA expression of TLR2/4, iNOS, IP-10, IL-1 $\beta$ , IL-6, and IL-10, in both sexes. These findings agree with published data in unsexed astrocytes showing that LPS activates astrocytes through TLR2 and TLR4, promoting classical immune functions in astrocytes such as the increase of pro-inflammatory cytokines and

chemokines expression (Rodgers et al., 2020). It is noteworthy that the response of female astrocytes to LPS is significantly greater than that of male ones with respect to iNOS, IL-6, and IL-10 expression, being the TLR4 expression similar in both sexes. It has been previously shown by us and others that the NF- $\kappa$ B pathway mediates astrocytic pro-inflammatory response to LPS (Bellini et al., 2011; Cerciati et al., 2010). To prevent excessive X-chromosome responses in women, one of the two X-chromosomes is inactivated. However, 15% of the X genes escape inactivation, and their copy number is higher in women than in men (Mousavi et al., 2020). Several protein members of the toll-like receptor (TLR) signaling cascade, including members of NF- $\kappa$ B signaling pathway, are encoded on the X chromosome on the XCI escaping sites (Y. Li et al., 2020). Consequently, in females the two sets of X-linked parental genes, with different regulatory and activation capacity could represent a more balanced female immune response to infectious agents through the involvement of X-linked genes. Since a controlled innate immune response is beneficial to resolve inflammation, this could account for a better prognosis for women against infectious diseases (Gay et al., 2021).

Treatment of primary astrocytes with IGF-1 reversed the effect of LPS on TLR4 mRNA levels in both sexes, in agreement with a previous work made in unsexed astrocyte cultures (Bellini et al., 2011) which showed that IGF-1 reduces the effects of LPS on astrocytes by decreasing the expression of TLR4 and consequent deactivation of NF- $\kappa$ B that mediated transcription of proinflammatory cytokines. However, in the present study we found that IGF-1 blocked the effect of LPS on IL-1 $\beta$ , IL-6, and IL-10 expression only in male astrocytes. Neuroprotective and anti-inflammatory effects of IGF-1 have been described using unsexed cultures (Acáz-Fonseca et al., 2019; Bellini et al., 2011) or male animals exclusively (Madathil et al., 2013; Montivero et al., 2021). The novelty of our data is that we reveal that IGF-1 do not show anti-inflammatory effects in females. These findings could clarify the controversial results obtained when evaluating the effects of IGF-1 on neuroinflammation regardless of sex (Fernandez & Torres-Alemán, 2012; Labandeira-García et al., 2017). We may hypothesize that IGF-1 is not able to counteract the LPS inflammatory effect in females due to higher expression of NF- $\kappa$ B signaling X-linked genes. Nevertheless, further studies using the four-core genotype transgenic model (Cabrera Zapata et al., 2021) are required to establish direct causative mechanisms.

Under injury or infection, brain astrocytes are activated not only to express neurotrophic and proinflammatory factors but also to remove denatured proteins and cell debris to facilitate tissue repair. In this study, we set out to analyze the influence of sex on the actions of IGF-1 in astrocytic phagocytosis. Our results indicate that, under basal conditions, astrocytes from primary female cultures have higher phagocytic activity than male ones, in agreement with what has been published for microglia and peripheral immune cells (Gassen et al., 2021; N. Yanguas-Casás et al., 2020; Natalia Yanguas-Casás et al., 2018). As we have previously shown, phagocytosis of brain-derived cellular debris was stimulated by LPS treatment in cultured male astrocytes but inhibited in female cells (Crespo-Castrillo et al., 2020). Our present results also reveal that IGF-1 counteracts

the effect of LPS on neural debris phagocytosis only in male LPS-stimulated astrocytes, which may be due to sex-differences in IGF-1 signaling.

One of the most relevant results of this study is the observed basal sexual difference in AKT-phosphorylation in astrocytes. Neither male nor female astrocytes showed an LPS effect on p-AKT levels. However, IGF-1 was able to increase p-AKT both in resting and inflammatory conditions, only in male astrocytes. In addition, blocking the pathway by using three PI3K inhibitors with selectivity toward p110 catalytic isoforms, p110 $\alpha$ , p110 $\beta$ , and p110 $\delta$ , results in a significant decrease in the levels of phosphorylation of AKT with respect to the group treated with LPS plus IGF-1, only in males. These results show for the first time that while PI3K activity is higher in female astrocytes, its activation by IGF-1 is greater in male than in female and this action is specific for IGF-1 since EGF, a known stimulator of AKT phosphorylation through PI3K activation, induced an increase in pAKT in both sexes. IGF-1R levels were similar in both sexes and the receptor co-immunoprecipitated with the three p110 isoforms, indicating that all of them participate in the phosphorylation of AKT, which is consistent with other studies in various cell types (Chaussade et al., 2007; Wahane et al., 2014). There are no data in the literature showing sex differences in the expression and roles of individual p110 isoforms in astrocytes. Here we show that the expression levels of the three p110 isoforms were higher in male astrocytes, although the difference was statistically significant only for p110 $\alpha$ . These differences could explain at least in part the different actions of IGF-1 on the AKT phosphorylation in male and female astrocytes. Furthermore, AKT phosphorylation is also regulated by the actions of phosphatases such as the phosphatase and tensin homolog deleted on chromosome 10 (PTEN), that dephosphorylates phosphatidylinositol 3,4,5-triphosphate (PIP3) and thereby inhibits the PI3K/AKT kinase pathway (Arevalo & Rodríguez-Tébar, 2006) and a study indicated that overexpression of PTEN in astrocytes promotes inflammatory responses (Guan et al., 2021). Other work showed that PTEN expression and activity are reduced in women muscle compared with men (Samaan et al., 2015). It is not known whether astrocytic PTEN expression is also sex-specific but we could speculate that higher level of AKT phosphorylation and in turn higher phagocytosis and inflammatory response observed in female astrocyte may be due to a different PTEN activity. In addition, it has been reported a homeostatic regulation of PTEN by PI3K in astrocytes modulated by IGF-1 (Fernández et al., 2008). The higher basal astrocytic AKT phosphorylation observed in females suggests an intrinsic regulation that causes their insensitivity to exogenous IGF-1. Additional studies are necessary to validate this hypothesis. So far, few data provide information on PI3K-p110-subtype-specific functions in the CNS and there are no publications on functions of PI3K- p110 $\alpha$  in neuroinflammation. In this study we report that only p110 $\alpha$  subunit is involved in the actions of IGF-1 on inflammatory response and phagocytic activity of reactive male astrocytes. Data obtained support this hypothesis, since there is no IGF-1 effect on female astrocytic inflammation and phagocytosis. Therefore, the lack of effects of IGF-1 on female astrocytic phagocytosis may be explained by the lower expression p110 $\alpha$ .

It is noteworthy that despite all three p110 isoforms are involved in the IGF-1-mediated AKT phosphorylation, only p110 $\alpha$  is implicated in the anti-inflammatory and phagocytic actions of IGF-1, as IGF-1 is still able to prevent LPS-induced inflammation and phagocytosis in astrocytes even under conditions of AKT-phosphorylation blockade by p110 $\beta$  and p110 $\delta$  inhibitors. Some evidence suggests that IGF-1 is capable of preventing H<sub>2</sub>O<sub>2</sub>-induced apoptosis in myoblasts, through an AKT- and MEK-independent, but p110 $\alpha$ -dependent mechanism (Matheny Jr. & Adamo, 2010). Considering that there are other kinases also regulated by p110 $\alpha$  in response to IGF-1, it is possible that one or more may contribute to the effects observed here.

Overall, we showed that IGF-1 plays a sex-specific role in modulating neuroinflammation triggered by LPS, decreasing phagocytosis and the release of proinflammatory factors in reactive male astrocytes. We previously established that the effect of LPS on phagocytosis is different in male and female cells. The current work extends this to show that IGF-1 decreases phagocytosis only in males, likely to reduce the exacerbated response. The observed effects of IGF-1 were mediated by activation of PI3K signaling pathway. Sex-differences observed in the actions of IGF-1 on AKT-phosphorylation, inflammation and phagocytosis of astrocytes populations are suggestive of differences in p110 isoforms expression and provide an interesting opportunity for further research.

#### ACKNOWLEDGMENTS

We thank Elisa Baidés Rosell for excellent technical assistance. This work was supported by grants BFU2017-82754-R and PID2020-115019RB-I00 from Agencia Estatal de Investigación (AEI), co-funded by Fondo Europeo de Desarrollo Regional (FEDER) and by Centro de Investigación Biomédica en Red de Fragilidad y Envejecimiento Saludable (CIBERFES), Instituto de Salud Carlos III, Madrid, Spain.

#### CONFLICT OF INTEREST

The authors declare no potential conflict of interest.

#### AUTHOR CONTRIBUTIONS

Maria-Angeles Arevalo and Daniel Pinto-Benito conceived and designed the study and analyzed and interpreted the data. Daniel Pinto-Benito, Carmen Paradela-Leal, Danny Ganchala, and Paula de Castro-Molina conducted the experimental procedures. Daniel Pinto-Benito elaborated figures and Maria-Angeles Arevalo wrote the first draft of the manuscript. All authors contributed to manuscript revision and approved the final version.

#### DATA AVAILABILITY STATEMENT

The data that support the findings of this study are available from D.P.B. and M.A.A. upon reasonable request.

#### ORCID

Daniel Pinto-Benito  <https://orcid.org/0000-0001-8321-4546>

Maria-Angeles Arevalo  <https://orcid.org/0000-0002-4303-9576>

## REFERENCES

- Acac-Fonseca, E., Duran, J. C., Carrero, P., Garcia-Segura, L. M., & Arevalo, M. A. (2015). Sex differences in glia reactivity after cortical brain injury. *Glia*, 63(11), 1966–1981. <https://doi.org/10.1002/glia.22867>
- Acac-Fonseca, E., Ortiz-Rodriguez, A., Azcoitia, I., Garcia-Segura, L. M., & Arevalo, M.-A. (2019). Notch signaling in astrocytes mediates their morphological response to an inflammatory challenge. *Cell Death Discovery*, 5(1), 85. <https://doi.org/10.1038/s41420-019-0166-6>
- Anderson, M. A., Ao, Y., & Sofroniew, M. V. (2014). Heterogeneity of reactive astrocytes. *Neuroscience Letters*, 565, 23–29. <https://doi.org/10.1016/j.neulet.2013.12.030>
- Arevalo, M.-A., Azcoitia, I., & Garcia-Segura, L. M. (2015). The neuroprotective actions of oestradiol and oestrogen receptors. *Nature Reviews Neuroscience*, 16(1), 17–29. <https://doi.org/10.1038/nrn3856>
- Arevalo, M.-A., & Rodriguez-Tébar, A. (2006). Activation of casein kinase II and inhibition of phosphatase and tensin homologue deleted on chromosome 10 phosphatase by nerve growth factor/p75NTR inhibit glycogen synthase kinase-3beta and stimulate axonal growth. *Molecular Biology of the Cell*, 17(8), 3369–3377. <https://doi.org/10.1091/mbc.e05-12-1144>
- Bellesi, M., de Vivo, L., Chini, M., Gilli, F., Tononi, G., & Cirelli, C. (2017). Sleep loss promotes astrocytic phagocytosis and microglial activation in mouse cerebral cortex. *The Journal of Neuroscience*, 37(21), 5263–5273. <https://doi.org/10.1523/jneurosci.3981-16.2017>
- Bellini, M. J., Hereñú, C. B., Goya, R. G., & Garcia-Segura, L. M. (2011). Insulin-like growth factor-I gene delivery to astrocytes reduces their inflammatory response to lipopolysaccharide. *Journal of Neuroinflammation*, 8, 21–21. <https://doi.org/10.1186/1742-2094-8-21>
- Bösch, F., Angele, M. K., & Chaudry, I. H. (2018). Gender differences in trauma, shock and sepsis. *Military Medical Research*, 5(1), 35. <https://doi.org/10.1186/s40779-018-0182-5>
- Brown, J., Wang, H., Suttles, J., Graves, D. T., & Martin, M. (2011). Mammalian target of rapamycin complex 2 (mTORC2) negatively regulates Toll-like receptor 4-mediated inflammatory response via FoxO1. *Journal of Biological Chemistry*, 286(52), 44295–44305. <https://doi.org/10.1074/jbc.M111.245951>
- Bsibsi, M., Ravid, R., Gveric, D., & van Noort, J. M. (2002). Broad expression of Toll-like receptors in the human central nervous system. *Journal of Neuropathology & Experimental Neurology*, 61(11), 1013–1021. <https://doi.org/10.1093/jnen/61.11.1013>
- Cabrera Zapata, L. E., Cisternas, C. D., Sosa, C., Garcia-Segura, L. M., Arevalo, M. A., & Cambiasso, M. J. (2021). X-linked histone H3K27 demethylase Kdm6a regulates sexually dimorphic differentiation of hypothalamic neurons. *Cellular and Molecular Life Sciences*, 78(21–22), 7043–7060. <https://doi.org/10.1007/s00018-021-03945-0>
- Castro, J., Garcia, R. I., Kwok, S., Banerjee, A., Petravicz, J., Woodson, J., Mellios, N., Tropea, D., & Sur, M. (2014). Functional recovery with recombinant human IGF1 treatment in a mouse model of Rett syndrome. *Proceedings of the National Academy of Sciences of the United States of America*, 111(27), 9941–9946. <https://doi.org/10.1073/pnas.1311685111>
- Cerciat, M., Unkila, M., Garcia-Segura, L. M., & Arevalo, M.-A. (2010). Selective estrogen receptor modulators decrease the production of interleukin-6 and interferon-γ-inducible protein-10 by astrocytes exposed to inflammatory challenge in vitro. *Glia*, 58(1), 93–102. <https://doi.org/10.1002/glia.20904>
- Chaussade, C., Rewcastle, G. W., Kendall, J. D., Denny, W. A., Cho, K., Grønning, L. M., Chong, M. L., Anagnostou, S. H., Jackson, S. P., Daniele, N., & Shepherd, P. R. (2007). Evidence for functional redundancy of class IA PI3K isoforms in insulin signalling. *The Biochemical Journal*, 404(3), 449–458. <https://doi.org/10.1042/bj20070003>
- Chisholm, N. C., & Sohrabji, F. (2016). Astrocytic response to cerebral ischemia is influenced by sex differences and impaired by aging. *Neurobiology of Disease*, 85, 245–253. <https://doi.org/10.1016/j.nbd.2015.03.028>
- Chistyakov, D. V., Azbukina, N. V., Astakhova, A. A., Goriainov, S. V., Chistyakov, V. V., & Sergeeva, M. G. (2018). Sex-mediated differences in LPS induced alterations of TNFα, IL-10 expression, and prostaglandin synthesis in primary astrocytes. *International Journal of Molecular Sciences*, 19(9), 2793. <https://doi.org/10.3390/ijms19092793>
- Chung, W. S., Clarke, L. E., Wang, G. X., Stafford, B. K., Sher, A., Chakraborty, C., Joung, J., Foo, L. C., Thompson, A., Chen, C., Smith, S. J., & Barres, B. A. (2013). Astrocytes mediate synapse elimination through MEGF10 and MERTK pathways. *Nature*, 504(7480), 394–400. <https://doi.org/10.1038/nature12776>
- Chung, W. S., Verghese, P. B., Chakraborty, C., Joung, J., Hyman, B. T., Ulrich, J. D., Holtzman, D. M., & Barres, B. A. (2016). Novel allele-dependent role for APOE in controlling the rate of synapse pruning by astrocytes. *Proceedings of the National Academy of Sciences of the United States of America*, 113(36), 10186–10191. <https://doi.org/10.1073/pnas.1609896113>
- Crespo-Castrillo, A., Garcia-Segura, L.-M., & Arevalo, M.-A. (2020). The synthetic steroid tibolone exerts sex-specific regulation of astrocyte phagocytosis under basal conditions and after an inflammatory challenge. *Journal of Neuroinflammation*, 17(1), 37. <https://doi.org/10.1186/s12974-020-1719-6>
- Fernandez, A. M., & Torres-Alemán, I. (2012). The many faces of insulin-like peptide signalling in the brain. *Nature Reviews Neuroscience*, 13, 225. <https://doi.org/10.1038/nrn3209>
- Fernández, S., García-García, M., & Torres-Alemán, I. (2008). Modulation by insulin-like growth factor I of the phosphatase PTEN in astrocytes. *Biochimica et Biophysica Acta (BBA) - Molecular Cell Research*, 1783(5), 803–812. <https://doi.org/10.1016/j.bbamcr.2007.10.020>
- Fruman, D. A., Chiu, H., Hopkins, B. D., Bagrodia, S., Cantley, L. C., & Abraham, R. T. (2017). The PI3K pathway in human disease. *Cell*, 170(4), 605–635. <https://doi.org/10.1016/j.cell.2017.07.029>
- García-Segura, L. M., Arévalo, M.-A., & Azcoitia, I. (2010). Chapter 14 - Interactions of estradiol and insulin-like growth factor-I signalling in the nervous system: New advances. In L. Martini (Ed.), *Progress in Brain Research* (Vol. 181, pp. 251–272). Elsevier. <https://www.sciencedirect.com/science/article/pii/S007961230881014X>
- Gassen, J., White, J. D., Peterman, J. L., Mengelkoch, S., Proffitt Leyva, R. P., Prokosch, M. L., Eimerbrink, M. J., Brice, K., Cheek, D. J., Boehm, G. W., & Hill, S. E. (2021). Sex differences in the impact of childhood socioeconomic status on immune function. *Scientific Reports*, 11(1), 9827–9827. <https://doi.org/10.1038/s41598-021-89413-y>
- Gay, L., Melenotte, C., Lakbar, I., Mezouar, S., Devaux, C., Raoult, D., Bendiane, M. K., Leone, M., & Mège, J.-L. (2021). Sexual dimorphism and gender in infectious diseases. *Frontiers in Immunology*, 12(2973), 698121. <https://doi.org/10.3389/fimmu.2021.698121>
- Giatti, S., Diviccaro, S., Serafini, M. M., Caruso, D., Garcia-Segura, L. M., Viviani, B., & Melcangi, R. C. (2020). Sex differences in steroid levels and steroidogenesis in the nervous system: Physiopathological role. *Frontiers in Neuroendocrinology*, 56, 100804. <https://doi.org/10.1016/j.yfrne.2019.100804>
- Guan, X., Zhang, Y., Gareev, I., Beylerli, O., Li, X., Lu, G., Lv, L., & Hai, X. (2021). MiR-499a prevents astrocytes mediated inflammation in ischemic stroke by targeting PTEN. *Non-coding RNA Research*, 6(3), 146–152. <https://doi.org/10.1016/j.ncrna.2021.09.002>
- Hasel, P., Rose, I. V. L., Sadick, J. S., Kim, R. D., & Liddelow, S. A. (2021). Neuroinflammatory astrocyte subtypes in the mouse brain. *Nature Neuroscience*, 24(10), 1475–1487. <https://doi.org/10.1038/s41593-021-00905-6>
- Jaber, S. M., Bordt, E. A., Bhatt, N. M., Lewis, D. M., Gerecht, S., Fiskum, G., & Polster, B. M. (2018). Sex differences in the mitochondrial bioenergetics of astrocytes but not microglia at a physiologically



- relevant brain oxygen tension. *Neurochemistry International*, 117, 82–90. <https://doi.org/10.1016/j.neuint.2017.09.003>
- Jung, Y. J., & Chung, W. S. (2018). Phagocytic roles of glial cells in healthy and diseased brains. *Biomolecules & Therapeutics (Seoul)*, 26(4), 350–357. <https://doi.org/10.4062/biomolther.2017.133>
- Khasnavis, S., Jana, A., Roy, A., Mazumder, M., Bhushan, B., Wood, T., Ghosh, S., Watson, R., & Pahan, K. (2012). Suppression of nuclear factor- $\kappa$ B activation and inflammation in microglia by physically modified saline\*. *Journal of Biological Chemistry*, 287(35), 29529–29542. <https://doi.org/10.1074/jbc.M111.338012>
- Kondo, Y., Miyazato, A., Okamoto, K., & Tanaka, H. (2021). Impact of sex differences on mortality in patients with sepsis after trauma: A nationwide cohort study. *Frontiers in Immunology*, 12(2573), 678157. <https://doi.org/10.3389/fimmu.2021.678156>
- Labandeira-García, J. L., Costa-Besada, M. A., Labandeira, C. M., Villar-Cheda, B., & Rodríguez-Perez, A. I. (2017). Insulin-like growth factor-1 and neuroinflammation. *Frontiers in Aging Neuroscience*, 9, 365. <https://doi.org/10.3389/fnagi.2017.00365>
- Leite, J. A., Isaksen, T. J., Heuck, A., Scavone, C., & Lykke-Hartmann, K. (2020). The  $\alpha$ (2) Na(+)/K(+)-ATPase isoform mediates LPS-induced neuroinflammation. *Scientific Reports*, 10(1), 14180–14180. <https://doi.org/10.1038/s41598-020-71027-5>
- Li, W., Ali, T., Zheng, C., Liu, Z., He, K., Shah, F. A., Ren, Q., Rahman, S. U., Li, N., Yu, Z. J., & Li, S. (2021). Fluoxetine regulates eEF2 activity (phosphorylation) via HDAC1 inhibitory mechanism in an LPS-induced mouse model of depression. *Journal of Neuroinflammation*, 18(1), 38. <https://doi.org/10.1186/s12974-021-02091-5>
- Li, Y., Jerkic, M., Slutsky, A. S., & Zhang, H. (2020). Molecular mechanisms of sex bias differences in COVID-19 mortality. *Critical Care*, 24(1), 405. <https://doi.org/10.1186/s13054-020-03118-8>
- Liddelow, S. A., Guttenplan, K. A., Clarke, L. E., Bennett, F. C., Bohlen, C. J., Schirmer, L., Bennett, M. L., Münch, A. E., Chung, W.-S., Peterson, T. C., Wilton, D. K., Frouin, A., Napier, B. A., Panicker, N., Kumar, M., Buckwalter, M. S., Rowitch, D. H., Dawson, V. L., Dawson, T. M., ... Barres, B. A. (2017). Neurotoxic reactive astrocytes are induced by activated microglia. *Nature*, 541, 481. <https://doi.org/10.1038/nature21029>, <https://www.nature.com/articles/nature21029#supplementary-information>
- Madathil, S. K., Carlson, S. W., Brelsfoard, J. M., Ye, P., D'Ercole, A. J., & Saatman, K. E. (2013). Astrocyte-specific overexpression of insulin-like growth factor-1 protects hippocampal neurons and reduces behavioral deficits following traumatic brain injury in mice. *PLoS One*, 8(6), e67204. <https://doi.org/10.1371/journal.pone.0067204>
- Matheny, R. W., Jr., & Adamo, M. L. (2010). PI3K p110 alpha and p110 beta have differential effects on Akt activation and protection against oxidative stress-induced apoptosis in myoblasts. *Cell Death and Differentiation*, 17(4), 677–688. <https://doi.org/10.1038/cdd.2009.150>
- McGowan, J. E., Jr., Barnes, M. W., & Finland, M. (1975). Bacteremia at Boston City Hospital: Occurrence and mortality during 12 selected years (1935-1972), with special reference to hospital-acquired cases. *The Journal of Infectious Diseases*, 132(3), 316–335. <https://doi.org/10.1093/infdis/132.3.316>
- Mendez, P., Azcoitia, I., & Garcia-Segura, L. M. (2003). Estrogen receptor alpha forms estrogen-dependent multimolecular complexes with insulin-like growth factor receptor and phosphatidylinositol 3-kinase in the adult rat brain. *Molecular Brain Research*, 112(1), 170–176. [https://doi.org/10.1016/S0169-328X\(03\)00088-3](https://doi.org/10.1016/S0169-328X(03)00088-3)
- Montivero, A. J., Ghersi, M. S., Silvero, C. M. J., Artur de la Villarmois, E., Catalan-Figueroa, J., Herrera, M., Becerra, M. C., Hereñú, C. B., & Pérez, M. F. (2021). Early IGF-1 gene therapy prevented oxidative stress and cognitive deficits induced by traumatic brain injury. *Frontiers in Pharmacology*, 12, 672392–672392. <https://doi.org/10.3389/fphar.2021.672392>
- Morizawa, Y. M., Hirayama, Y., Ohno, N., Shibata, S., Shigetomi, E., Sui, Y., Nabekura, J., Sato, K., Okajima, F., Takebayashi, H., Okano, H., & Koizumi, S. (2017). Reactive astrocytes function as phagocytes after brain ischemia via ABCA1-mediated pathway. *Nature Communications*, 8(1), 28. <https://doi.org/10.1038/s41467-017-00037-1>
- Morrison, H. W., & Filosa, J. A. (2016). Sex differences in astrocyte and microglia responses immediately following middle cerebral artery occlusion in adult mice. *Neuroscience*, 339, 85–99. <https://doi.org/10.1016/j.neuroscience.2016.09.047>
- Mousavi, M. J., Mahmoudi, M., & Ghotloo, S. (2020). Escape from X chromosome inactivation and female bias of autoimmune diseases. *Molecular Medicine*, 26(1), 127. <https://doi.org/10.1186/s10020-020-00256-1>
- Nguyen, J. V., Soto, I., Kim, K.-Y., Bushong, E. A., Oglesby, E., Valiente-Soriano, F. J., Yang, Z., Davis, C. H., Bedont, J. L., Son, J. L., Wei, J. O., Buchman, V. L., Zack, D. J., Vidal-Sanz, M., Ellisman, M. H., & Marsh-Armstrong, N. (2011). Myelination transition zone astrocytes are constitutively phagocytic and have synuclein dependent reactivity in glaucoma. *Proceedings of the National Academy of Sciences of the United States of America*, 108(3), 1176–1181. <https://doi.org/10.1073/pnas.1013965108>
- O'Connor, J. C., McCusker, R. H., Strle, K., Johnson, R. W., Dantzer, R., & Kelley, K. W. (2008). Regulation of IGF-I function by proinflammatory cytokines: At the interface of immunology and endocrinology. *Cellular Immunology*, 252(1–2), 91–110. <https://doi.org/10.1016/j.cellimm.2007.09.010>
- Park, S.-E., Dantzer, R., Kelley, K. W., & McCusker, R. H. (2011). Central administration of insulin-like growth factor-I decreases depressive-like behavior and brain cytokine expression in mice. *Journal of Neuroinflammation*, 8, 12–12. <https://doi.org/10.1186/1742-2094-8-12>
- Pfaffl, M. W., Tichopad, A., Prgomet, C., & Neuvians, T. P. (2004). Determination of stable housekeeping genes, differentially regulated target genes and sample integrity: BestKeeper – Excel-based tool using pairwise correlations. *Biotechnology Letters*, 26(6), 509–515. <https://doi.org/10.1023/B:BILE.0000019559.84305.47>
- Ponath, G., Ramanan, S., Mubarak, M., Housley, W., Lee, S., Sahinkaya, F. R., Vortmeyer, A., Raine, C. S., & Pitt, D. (2017). Myelin phagocytosis by astrocytes after myelin damage promotes lesion pathology. *Brain*, 140(2), 399–413. <https://doi.org/10.1093/brain/aww298>
- Pons, S., & Torres-Aleman, I. (2000). Insulin-like growth factor-I stimulates dephosphorylation of I $\kappa$ B through the serine phosphatase calcineurin (protein phosphatase 2B). *Journal of Biological Chemistry*, 275(49), 38620–38625. <https://doi.org/10.1074/jbc.M004531200>
- Porcher, L., Bruckmeier, S., Burbano, S. D., Finnell, J. E., Gorny, N., Klett, J., Wood, S. K., & Kelly, M. P. (2021). Aging triggers an upregulation of a multitude of cytokines in the male and especially the female rodent hippocampus but more discrete changes in other brain regions. *Journal of Neuroinflammation*, 18(1), 219. <https://doi.org/10.1186/s12974-021-02252-6>
- Pridham, K. J., le, L., Guo, S., Varghese, R. T., Algino, S., Liang, Y., Fajardin, R., Rodgers, C. M., Simonds, G. R., Kelly, D. F., & Sheng, Z. (2018). PIK3CB/p110 $\beta$  is a selective survival factor for glioblastoma. *Neuro-Oncology*, 20(4), 494–505. <https://doi.org/10.1093/neuonc/nox181>
- Reinhardt, R. R., & Bondy, C. A. (1994). Insulin-like growth factors cross the blood-brain barrier. *Endocrinology*, 135(5), 1753–1761. <https://doi.org/10.1210/endo.135.5.7525251>
- Rodgers, K. R., Lin, Y., Langan, T. J., Iwakura, Y., & Chou, R. C. (2020). Innate immune functions of astrocytes are dependent upon tumor necrosis factor- $\alpha$ . *Scientific Reports*, 10(1), 7047–7047. <https://doi.org/10.1038/s41598-020-63766-2>
- Samaan, M. C., Anand, S. S., Sharma, A. M., Samjoo, I. A., & Tarnopolsky, M. A. (2015). Sex differences in skeletal muscle phosphatase and tensin homolog deleted on chromosome 10 (PTEN) levels: A cross-sectional study. *Scientific Reports*, 5, 9154–9154. <https://doi.org/10.1038/srep09154>
- Santi, A., Genis, L., & Torres Aleman, I. (2018). A coordinated action of blood-borne and brain insulin-like growth factor I in the response to



- traumatic brain injury. *Cerebral Cortex*, 28(6), 2007–2014. <https://doi.org/10.1093/cercor/bhx106>
- Sofroniew, M. V., & Vinters, H. V. (2010). Astrocytes: Biology and pathology. *Acta Neuropathologica*, 119(1), 7–35. <https://doi.org/10.1007/s00401-009-0619-8>
- Tang, B., Song, M., Xie, X., Le, D., Tu, Q., Wu, X., & Chen, M. (2021). Tumor necrosis factor-stimulated Gene-6 (TSG-6) secreted by BMSCs regulates activated astrocytes by inhibiting NF- $\kappa$ B signaling pathway to ameliorate blood brain barrier damage after intracerebral hemorrhage. *Neurochemical Research*, 46, 2387–2402. <https://doi.org/10.1007/s11064-021-03375-1>
- Tapia-Gonzalez, S., Carrero, P., Pernia, O., Garcia-Segura, L. M., & Diz-Chaves, Y. (2008). Selective oestrogen receptor (ER) modulators reduce microglia reactivity in vivo after peripheral inflammation: Potential role of microglial ERs. *The Journal of Endocrinology*, 198(1), 219–230. <https://doi.org/10.1677/joe-07-0294>
- Vilalta, A., & Brown, G. C. (2018). Neurophagy, the phagocytosis of live neurons and synapses by glia, contributes to brain development and disease. *The FEBS Journal*, 285(19), 3566–3575. <https://doi.org/10.1111/febs.14323>
- Villarreal, A., Vidos, C., Monteverde Busso, M., Cieri, M. B., & Ramos, A. J. (2021). Pathological neuroinflammatory conversion of reactive astrocytes is induced by microglia and involves chromatin remodeling. *Frontiers in Pharmacology*, 12, 689346–689346. <https://doi.org/10.3389/fphar.2021.689346>
- Wahane, S. D., Hellbach, N., Prentzell, M. T., Weise, S. C., Vezzali, R., Kreutz, C., Timmer, J., Kriegelstein, K., Thedieck, K., & Vogel, T. (2014). PI3K-p110-alpha-subtype signalling mediates survival, proliferation and neurogenesis of cortical progenitor cells via activation of mTORC2. *Journal of Neurochemistry*, 130(2), 255–267. <https://doi.org/10.1111/jnc.12718>
- Wang, F., Wang, L., Wang, Y., Li, D., Hu, T., Sun, M., & Lei, P. (2020). Exogenous IGF-1 improves cognitive function in rats with high-fat diet consumption. *Journal of Molecular Endocrinology*, 64(2), 115–123. <https://doi.org/10.1530/jme-19-0150>
- Witkowska-Sędek, E., & Pyrzak, B. (2020). Chronic inflammation and the growth hormone/insulin-like growth factor-1 axis. *Central European Journal of Immunology*, 45(4), 469–475. <https://doi.org/10.5114/ceji.2020.103422>
- Yanguas-Casás, N., Crespo-Castrillo, A., Arevalo, M. A., & Garcia-Segura, L. M. (2020). Aging and sex: Impact on microglia phagocytosis. *Aging Cell*, 19(8), e13182. <https://doi.org/10.1111/accel.13182>
- Yanguas-Casás, N., Crespo-Castrillo, A., de Ceballos, M. L., Chowen, J. A., Azcoitia, I., Arevalo, M. A., & Garcia-Segura, L. M. (2018). Sex differences in the phagocytic and migratory activity of microglia and their impairment by palmitic acid. *Glia*, 66(3), 522–537. <https://doi.org/10.1002/glia.23263>
- Yuan, L.-J., Zhang, M., Chen, S., & Chen, W.-F. (2021). Anti-inflammatory effect of IGF-1 is mediated by IGF-1R cross talk with GPER in MPTP/MPP<sup>+</sup>-induced astrocyte activation. *Molecular and Cellular Endocrinology*, 519, 111053. <https://doi.org/10.1016/j.mce.2020.111053>

**How to cite this article:** Pinto-Benito, D., Paradela-Leal, C., Ganchala, D., de Castro-Molina, P., & Arevalo, M.-A. (2022). IGF-1 regulates astrocytic phagocytosis and inflammation through the p110 $\alpha$  isoform of PI3K in a sex-specific manner. *Glia*, 70(6), 1153–1169. <https://doi.org/10.1002/glia.24163>